

The Terminating-Knockoff Filter: Fast High-Dimensional Variable Selection with False Discovery Rate Control

Jasin Machkour*

*Department of Electrical Engineering and Information Technology
Technische Universität Darmstadt
Darmstadt, Germany*

J.MACHKOUR@SPG.TU-DARMSTADT.DE

Michael Muma

*Department of Electrical Engineering and Information Technology
Technische Universität Darmstadt
Darmstadt, Germany*

MUMA@SPG.TU-DARMSTADT.DE

Daniel P. Palomar

*Department of Electronic and Computer Engineering
Department of Industrial Engineering and Data Analytics
The Hong Kong University of Science and Technology
Clear Water Bay, Hong Kong*

PALOMAR@UST.HK

Editor: TBD

Abstract

We propose the Terminating-Knockoff (T-Knock) filter, a fast variable selection method for high-dimensional data. The T-Knock filter controls a user-defined target false discovery rate (FDR) while maximizing the number of selected true positives. This is achieved by fusing the solutions of multiple early terminated random experiments. The experiments are conducted on a combination of the original data and multiple sets of randomly generated knockoff variables. A finite sample proof based on martingale theory for the FDR control property is provided. Numerical simulations show that the FDR is controlled at the target level while allowing for a high power. We prove under mild conditions that the knockoffs can be sampled from any univariate distribution. The computational complexity of the proposed method is derived and it is demonstrated via numerical simulations that the sequential computation time is multiple orders of magnitude lower than that of the strongest benchmark methods in sparse high-dimensional settings. The T-Knock filter outperforms state-of-the-art methods for FDR control on a simulated genome-wide association study (GWAS), while its computation time is more than two orders of magnitude lower than that of the strongest benchmark methods.

Keywords: T-Knock filter, false discovery rate (FDR) control, high-dimensional variable selection, martingale theory, genome-wide association studies.

1. Introduction and Motivation

We consider the task of selecting only those variables that are truly related to a given response from a potentially high-dimensional set of candidate variables, where the number of candidates may exceed the number of observations. In such settings it is desirable that the proportion of falsely selected variables among all selected variables is low while the proportion of correctly selected variables is high. The expected values of these quantities are referred to as the false discovery rate (FDR) and the true positive rate (TPR), respectively. The FDR and TPR are expressed mathematically

*. Corresponding author.

as follows: Given the index set of the active variables $\mathcal{A} \subseteq \{1, \dots, p\}$, where p is the number of candidate variables (i.e., potential explanatory variables), and the index set of the selected active variables $\widehat{\mathcal{A}} \subseteq \{1, \dots, p\}$, the FDR and the TPR are defined by

$$\text{FDR} := \mathbb{E} \left[\frac{|\widehat{\mathcal{A}} \setminus \mathcal{A}|}{1 \vee |\widehat{\mathcal{A}}|} \right] \quad \text{and} \quad \text{TPR} := \mathbb{E} \left[\frac{|\mathcal{A} \cap \widehat{\mathcal{A}}|}{1 \vee |\mathcal{A}|} \right], \quad (1)$$

respectively, where $|\cdot|$ denotes the cardinality operator and the symbol \vee stands for the maximum operator, i.e., $a \vee b = \max\{a, b\}$, $a, b \in \mathbb{R}$.¹ Note that by definition the FDR and TPR are zero when $|\widehat{\mathcal{A}}| = 0$ and $|\mathcal{A}| = 0$, respectively. While the FDR and the TPR of an oracle variable selection procedure are 0% and 100%, respectively, in practice, a tradeoff must be accomplished. In many practical high-dimensional applications, where the number of explanatory variables p exceeds the number of observations n , only a few of the explanatory variables are related to the response variable. Our aim is to discover as many as possible of these few active variables while guaranteeing that the FDR is controlled at the target level. In order to express the assumed linear relationship between the explanatory variables and the response variable, the linear regression model is considered. It is defined by

$$\mathbf{y} = \mathbf{X}\boldsymbol{\beta} + \boldsymbol{\epsilon}, \quad (2)$$

where $\mathbf{X} = [\mathbf{x}_1 \ \mathbf{x}_2 \ \dots \ \mathbf{x}_p]$ with $\mathbf{x}_j \in \mathbb{R}^n$, $j = 1, \dots, p$, is the fixed predictor matrix containing p predictors and n observations, $\mathbf{y} \in \mathbb{R}^n$ is the response vector, $\boldsymbol{\beta} \in \mathbb{R}^p$ is the parameter vector, and $\boldsymbol{\epsilon} \sim \mathcal{N}(\mathbf{0}, \sigma^2 \mathbf{I})$, with \mathbf{I} being the identity matrix, is an additive Gaussian noise vector with noise level σ . Variables whose associated coefficients in $\boldsymbol{\beta}$ are non-zero (zero) are called actives or active variables (nulls or null variables).

In many real world applications, only a few variables among tens of thousands, or even a few millions, are truly associated with the response. For example, in genome-wide association studies (GWAS) only a few common genetic variations called single nucleotide polymorphisms (SNPs) are associated with a phenotype of interest (Buniello et al., 2019). In this application, a low FDR is desired for two main reasons: First, for every potentially discovered influential SNP further extensive and expensive functional genomics studies and molecular biological laboratory experiments are needed to investigate whether the reported genetic associations are causal and to understand their functional implications (Chanock et al., 2007; Visscher et al., 2017; Huffman, 2018). However, the number of conducted follow-up functional genomics studies between 2005 and 2016 was roughly 98% lower compared to the discovered SNP-phenotype associations in GWAS (Gallagher and Chen-Plotkin, 2018). Thus, in order to not waste limited resources on researching false positives, a low FDR accompanied by a high TPR is desired. Second, the discoveries in a GWAS need to be reproducible in multiple studies conducted for other cohorts and/or populations before proceeding towards functional studies and laboratory experiments (Chanock et al., 2007). A low FDR certainly helps ensuring reproducibility.

There exist several FDR controlling methods in the literature. Popular classical methods are, e.g., the Benjamini-Hochberg (*BH*) method (Benjamini and Hochberg, 1995), the Benjamini-Yekutieli (*BY*) method (Benjamini and Yekutieli, 2001) whereas, e.g., the *fixed-X* knockoff method (Barber and Candès, 2015) and the *model-X* knockoff method (Candès et al., 2018) have been developed more recently. All these methods allow the user to specify a target FDR level that will implicitly determine how many and which variables are selected so as not to exceed the chosen target level.

1. Throughout this paper, the original definition of the FDR in (Benjamini and Hochberg, 1995) is used. Other definitions of the FDR, such as the positive FDR (Storey, 2003), exist. The interested reader is referred to both papers for discussions on different potential definitions of the FDR.

Note that there exist related lines of research that do not exclusively deal with FDR control but also other error measures in high-dimensional variable selection. Some of these lines of research are centered around stability selection methods (Meinshausen and Bühlmann, 2010; Shah and Samworth, 2013), data-splitting methods (Cox, 1975; Wasserman and Roeder, 2009; Meinshausen et al., 2009; Barber and Candès, 2019), and post-selection inference (Lockhart et al., 2014; Fithian et al., 2014; Lee et al., 2016; Tibshirani et al., 2016).

In this paper, we propose a new FDR controlling method called the Terminating-Knockoff (*T-Knock*) filter. The *T-Knock* filter is a fast and scalable tool that turns forward variable selection methods into FDR controlling methods. It builds upon the idea of using knockoffs as flagged null variables in the variable selection process (Miller, 1984, 2002; Wu et al., 2007; Barber and Candès, 2015; Candès et al., 2018) but it generates and/or utilizes knockoffs in a different manner than existing methods to provably control the FDR at the target level.

A high-level description of the *T-Knock* filter: It conducts multiple independent random experiments on the computer using the preferred forward selection procedure and, in each experiment, incorporates a different set of randomly generated knockoff variables of the same size and the same statistical properties into the predictor matrix. The knockoffs are easily generated by sampling from the univariate standard normal distribution. The forward selection process in each experiment is terminated early when selecting a distinct number of knockoff variables. Finally, the possibly differing sets of included candidate variables in each random experiment undergo a fusion process to obtain the estimated active set.

The most important advantages of the *T-Knock* filter are the following:

1. The *T-Knock* filter provably controls the FDR for any chosen target FDR level between 0% and 100%, even when p is much larger than n (i.e., high-dimensional setting).
2. Unlike existing knockoff methods, the knockoff generation process for the proposed *T-Knock* filter is data-independent and, therefore, does not require any information about the covariance structure of the candidate variables. This drastically reduces the required computation time for the generation of knockoffs when p is large.
3. The properties of the *T-Knock* filter, as stated in Point 1 and Point 2 above, rely only on mild and numerically validated assumptions.
4. The sequential computation time of the *T-Knock* filter in sparse high-dimensional settings is multiple orders of magnitude lower compared to that of the benchmark methods, such as the *model-X* knockoff method.
5. The computation time can be further reduced by using parallel processing on multicore computers. Moreover, a massive reduction is achieved with high performance clusters. This is possible because the random experiments of the *T-Knock* filter are independent of each other.
6. The tuning of the sparsity parameter for sparsity inducing methods, such as *Lasso* (Tibshirani, 1996), *LARS* (Efron et al., 2004), *elastic net* (Zou and Hastie, 2005), and *adaptive Lasso* (Zou, 2006), becomes unnecessary by incorporating these methods into the proposed *T-Knock* filter framework.

Notation: Throughout this paper, column vectors and matrices are denoted by boldface lowercase and boldface uppercase letters, respectively. Scalars are denoted by non-boldface lowercase or uppercase letters. With the exceptions of \mathcal{N} and \emptyset , which stand for the normal distribution and

the empty set, respectively, sets are denoted by calligraphic uppercase letters, e.g., \mathcal{A} with $|\mathcal{A}|$ denoting the associated cardinality. The symbols \mathbb{E} and Var denote the expectation and the variance operator, respectively. The terms “nulls” and “null variables” as well as the terms “knockoffs” and “knockoff variables” are used as synonyms, respectively.

Organization: The remainder of this paper is organized as follows: Section 2 introduces the methodology of the proposed *T-Knock* filter. Section 3 presents the main theoretical results regarding the properties of the proposed method, its algorithmic details, and its computational complexity. Section 4 discusses the results of numerical simulations while Section 5 evaluates the performances of the proposed *T-Knock* filter and the benchmark methods on a simulated genome-wide association study (GWAS). Section 6 concludes the paper. Technical proofs, numerical verification of assumptions, and additional simulations are deferred to the appendix.

2. The T-Knock Filter

In this section, the proposed *T-Knock* filter is introduced. First, high-dimensional variable selection methods that are used as building blocks of the *T-Knock* filter are briefly revisited. Then, the underlying methodology is described. Finally, the problem of calibrating the *T-Knock* filter to perform FDR control at the target level is formulated.

2.1 High-Dimensional Variable Selection Methods

Assuming that only a fraction of the p candidate variables is related to the response, that is, β contains only a few nonzero elements, it is reasonable to apply a sparsity inducing method to obtain a sparse estimate $\hat{\beta}$ of β . Some widely applied variable selection methods for high-dimensional and sparse regression are the *Lasso* (Tibshirani, 1996) and related methods, such as least angle regression (*LARS*) (Efron et al., 2004), the *adaptive Lasso* (Zou, 2006), the *elastic net* (Zou and Hastie, 2005), and the *fused Lasso* (Tibshirani et al., 2005). The *Lasso* solution is defined by

$$\hat{\beta}(\lambda) = \arg \min_{\beta} \|\mathbf{y} - \mathbf{X}\beta\|_2^2 + \lambda \|\beta\|_1, \quad (3)$$

where $\lambda > 0$ is a tuning parameter that controls the sparsity of the solution. In contrast, the *LARS* method does not optimize a closed form optimization problem but belongs to the class of forward-selection methods (Miller, 1984). The *LARS* algorithm starts with an empty set and adds one variable at a time to it by including the variable that has the highest correlation with the current residual. In each step, the coefficients of all selected variables are then linearly increased until the entry point of the next variable. The *Lasso* is closely related to the *LARS* method, since the solution path of the *Lasso* over λ is efficiently computed by applying a slightly modified *LARS* algorithm.² That is, instead of adding one variable at a time, the *Lasso* modification requires the removal of previously added variables when the associated coefficients change their sign. However, removed variables can enter the solution path again in later steps. Since the solution paths are terminated early by the *T-Knock* filter, there are only very few or even no zero crossings at all along the early terminated solution paths and, thus, in most cases *Lasso* and *LARS* produce very similar or the same solution paths when they are incorporated into the *T-Knock* filter. Therefore, throughout this paper, we will use the *LARS* algorithm to conduct the random experiments of the *T-Knock* filter.

2. An alternative approach to obtain the solution path of the *Lasso*, is to apply the pathwise coordinate descent algorithm (Friedman et al., 2007). It computes solution vectors for a grid of λ values.

2.2 The T-Knock Filter: Methodology

The general methodology underpinning the *T-Knock* filter consists of several steps that are illustrated in Figure 1. This section introduces the general framework and the notation which will be crucial for understanding why the *T-Knock* filter efficiently controls the FDR at the target level:

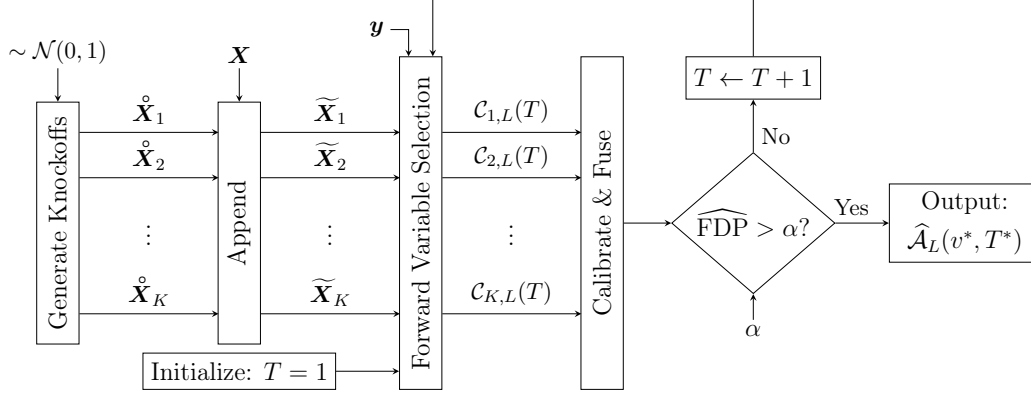


Figure 1: Simplified overview of the *T-Knock* filter framework: For each random experiment $k \in \{1, \dots, K\}$, the *T-Knock* filter generates a knockoff matrix $\mathring{\mathbf{X}}_k$ containing L knockoffs and appends it to \mathbf{X} to obtain the enlarged predictor matrix $\widetilde{\mathbf{X}}_k = [\mathbf{X} \ \mathring{\mathbf{X}}_k]$. With $\widetilde{\mathbf{X}}_k$ and the response \mathbf{y} as inputs, a forward variable selection method is applied to obtain the candidate sets $\mathcal{C}_{1,L}(T), \dots, \mathcal{C}_{K,L}(T)$, where T is iteratively increased from one until $\widehat{\text{FDP}}$ (i.e., an estimate of the proportion of false discoveries among all selected variables), that is determined by the calibration process, exceeds the target FDR level $\alpha \in [0, 1]$. Finally, a fusion procedure determines the selected active set $\widehat{\mathcal{A}}_L(v^*, T^*)$ for which the calibration procedure provides the optimal parameters T^* and v^* , such that the FDR is controlled at the target level α while maximizing the number of selected variables.

Step 1: Generate K , $K > 1$, knockoff matrices $\mathring{\mathbf{X}}_k$, $k = 1, \dots, K$, each containing L , $L \geq 1$, knockoff predictors. Every predictor within a knockoff matrix is sampled from a standard normal distribution.

Step 2: Append each knockoff matrix to the original predictor matrix \mathbf{X} , resulting in the enlarged predictor matrices

$$\widetilde{\mathbf{X}}_k := [\mathbf{X} \ \mathring{\mathbf{X}}_k] = [\mathbf{x}_1 \ \cdots \ \mathbf{x}_p \ \mathring{\mathbf{x}}_{k,1} \ \cdots \ \mathring{\mathbf{x}}_{k,L}], \quad k = 1, \dots, K,$$

where $\mathring{\mathbf{x}}_{k,1}, \dots, \mathring{\mathbf{x}}_{k,L}$ are the knockoffs. A visual illustration and summary of notation regarding the enlarged predictor matrices is provided in Figure 2.

Step 3: Apply a forward variable selection procedure, such as the *LARS* method, to $\{\widetilde{\mathbf{X}}_k, \mathbf{y}\}$, $k = 1, \dots, K$. For each random experiment, terminate the forward selection process after T , $T \geq 1$, knockoff variables are included. This results in the candidate active sets

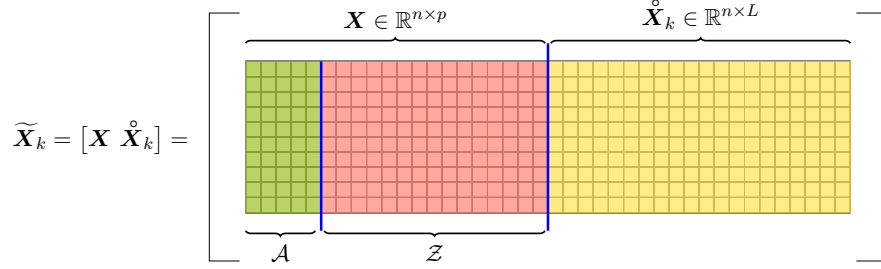


Figure 2: The enlarged predictor matrices $\widetilde{\mathbf{X}}_k$, $k = 1, \dots, K$, replace the original predictor matrix \mathbf{X} in each random experiment within the T -Knock filter framework. They contain the original and the knockoff predictors. The index set of the active variables and the index set of the null variables are denoted by \mathcal{A} and \mathcal{Z} , respectively.

$\mathcal{C}_{k,L}(T)$, $k = 1, \dots, K$.³ Note that after the forward selection process is terminated, all knockoffs are removed from the candidate active sets.

Step 4: Iteratively increase T and carry out Step 3 until $\widehat{\text{FDP}}$ (i.e., an estimate of the proportion of false discoveries among all selected variables), that is determined by the calibration process, exceeds the target FDR level $\alpha \in [0, 1]$. In addition to $\widehat{\text{FDP}}$, the calibration process also determines the optimal values v^* and T^* such that the FDR is controlled at the target level $\alpha \in [0, 1]$ while maximizing the number of selected variables.

Step 5: Fuse the candidate active sets to determine the estimator of the active set $\widehat{\mathcal{A}}_L(v^*, T^*)$. The fusion step is based on what we call the *relative occurrence*:

Definition 1 (Relative occurrence). *Let $K \in \mathbb{N}_+$ be the number of random experiments, $L \in \mathbb{N}_+$ the number of knockoffs, and $T \in \{1, \dots, L\}$ the number of included knockoffs after which the forward variable selection process in each random experiment is terminated. The relative occurrence of variable $j \in \{1, \dots, p\}$ is defined by*

$$\Phi_{T,L}(j) := \begin{cases} \frac{1}{K} \sum_{k=1}^K \mathbb{1}_k(j, T, L), & T \geq 1 \\ 0, & T = 0 \end{cases},$$

where $\mathbb{1}_k(j, T, L)$ is the indicator function for which

$$\mathbb{1}_k(j, T, L) = \begin{cases} 1, & j \in \mathcal{C}_{k,L}(T) \\ 0, & \text{otherwise} \end{cases}.$$

All variables whose relative occurrences at $T = T^*$ exceed the voting level $v^* \in [0.5, 1)$ are selected and the estimator of the active set is defined by

$$\widehat{\mathcal{A}}_L(v^*, T^*) := \{j : \Phi_{T^*,L}(j) > v^*\}. \quad (4)$$

3. Since we use the *LARS* method throughout this paper, variables can only be included but not dropped along the solution paths. Nevertheless, the T -Knock filter can also incorporate forward selection methods that remove some previously included variables from the candidate set along the solution path (e.g., *Lasso*). For such methods, the number of currently active knockoffs can decrease along the solution path. However, because the solution paths are terminated after T knockoffs are included for the first time, there is no ambiguity regarding the step in which the forward selection process ends.

The details of how the calibration process determines T^* , and v^* such that, for any choice of L , the *T-Knock* filter controls the FDR at the target level while maximizing the number of selected variables are deferred to Section 3.4. Moreover, an extension to the calibration process to jointly determine T^* , v^* , and L is also proposed in Section 3.4. The number of random experiments K is not subject to optimization. However choosing $K \geq 20$ provides excellent empirical results and we did not observe any notable improvements for $K \geq 100$ (see Section 4).⁴

The following example helps to develop some intuition about the three main ingredients of the *T-Knock* filter, which are

1. sampling knockoffs from the univariate standard normal distribution (see Figure 3),
2. early terminating the solution paths of the random experiments (see Figure 4), and
3. fusing the candidate sets based on their relative occurrences and a voting level $v \in [0.5, 1)$ (see Figure 5).

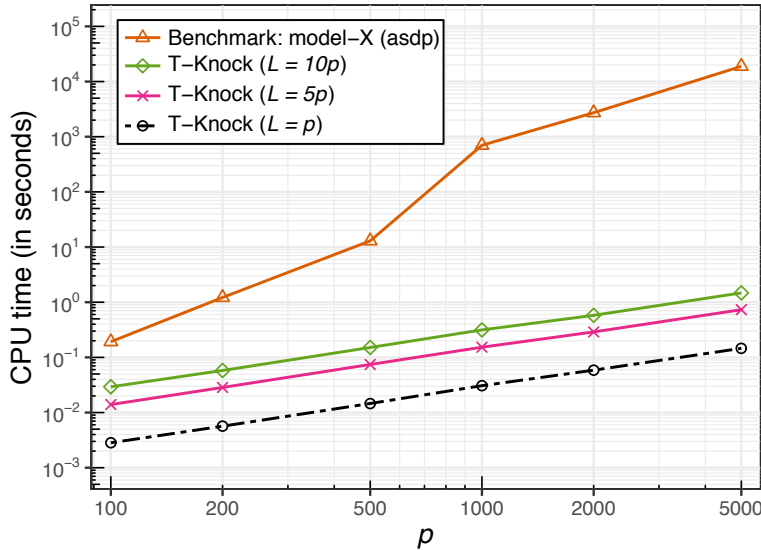
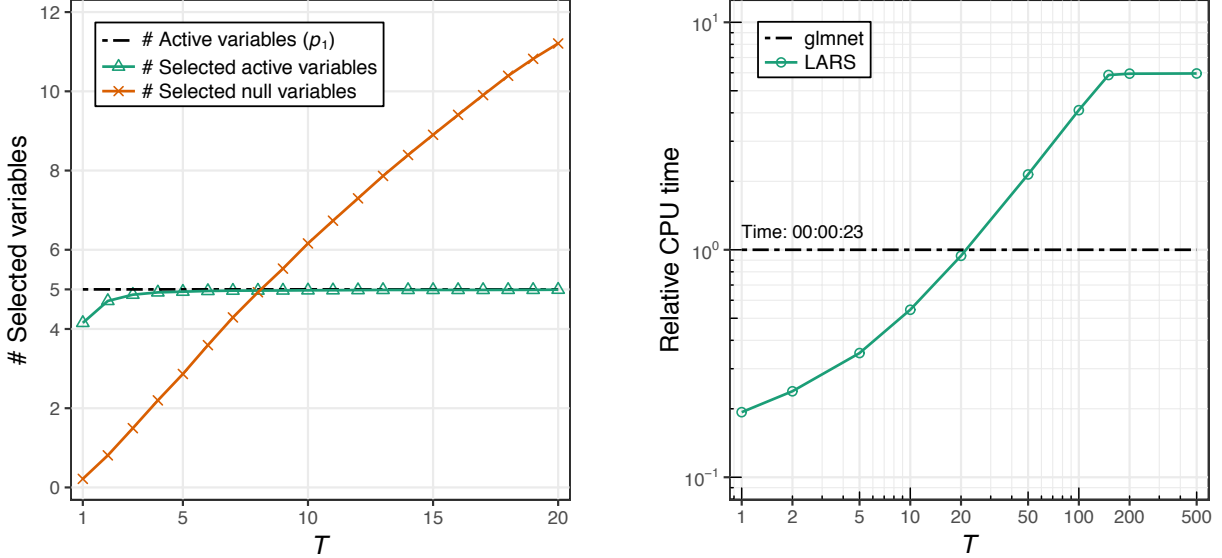


Figure 3: **Ingredient 1** - sampling knockoffs from the univariate standard normal distribution. The sequential computation time of generating one knockoff matrix for the proposed *T-Knock* filter is multiple orders of magnitude lower than that of the *model-X* knockoff method, which is a current benchmark. Note that for $p = 5000$ and $L = p$, the *T-Knock* knockoff generation process requires less than a second as compared to more than five hours for the *model-X* knockoff method. Even taking into account that the *T-Knock* filter requires, e.g., $K = 20$ of such knockoff matrices, its sequential computation time is still multiple orders of magnitude lower than that of the *model-X* knockoff method. The jump in computation time for the *model-X* knockoff method between $p = 500$ and $p = 1000$ is due to the suggestion of the authors to solve their proposed approximate semi-definite program (asdp) instead of their original semi-definite program for $p > 500$ in order to reduce the computation time required to generate *model-X* knockoffs. Note that both axes are scaled logarithmically. Setup: $n = 300$, $MC = 955$.⁵

4. Instead of fixing the number of random experiments, it could be increased until the relative occurrences $\Phi_{T,L}(j)$, $j = 1, \dots, p$, converge. However, since a massive reduction of computation time is achieved by executing the independent random experiments in parallel on multicore computers or high performance clusters, fixing K to a multiple of the available number of CPUs is preferable.

We generate sparse high-dimensional data sets with n observations and p predictors and a response that is generated by the linear model in (2). Further, $\beta_j = 1$ for active variables and $\beta_j = 0$ for null variables. The predictors are sampled from the standard normal distribution. The noise level σ is



(a) Number of selected variables vs. T . Setup: $n = 150$, $p = 300$, $p_1 = 5$, $v = 0.8$, $L = p$, $K = 20$, $\text{SNR} = 1$, $MC = 500$.

(b) The pathwise coordinate descent algorithm from the R package “glmnet” (Friedman et al., 2010) computing the *Lasso* on a λ -grid with 500 values and the terminated *LARS* algorithm. Note that both axes are scaled logarithmically. Setup: $n = 300$, $p = 50,000$, $p_1 = 5$, $L = p$, $\text{SNR} = 1$, $MC = 955$.

Figure 4: **Ingredient 2** - early terminating the solution paths of the random experiments. Figure (a) exemplifies that, on average, the number of selected active variables quickly increases towards the sparsity level p_1 (i.e., the number of active variables) and already for three included knockoffs almost all active variables are selected on average. However, the number of selected null variables also increases with increasing T . Figure (b) illustrates that even for $p = 50,000$ and $L = p$, when terminated early, the *LARS* algorithm (a fundamental building block of the *T-Knock* filter) is substantially faster than fitting the entire *Lasso* solution path using the pathwise coordinate descent algorithm for $2p$ variables as it is done by the *fixed-X* and *model-X* knockoff methods. Although the *T-Knock* filter needs to run the terminated *LARS* algorithm for, e.g., $K = 20$ random experiments within the *T-Knock filter*, its sequential computation time is still comparable to that of a single run of “glmnet” for low values of T and in ultra high-dimensional settings where p is much larger than n . Moreover, the independent random experiments can be run in parallel on multicore computers to achieve a substantial reduction in computation time. The “glmnet” computation time is used as the reference computation time and its absolute value is given above the reference line (format: hh:mm:ss). Note that after $T = 150$ knockoffs are included the computation time of the terminated *LARS* method does not increase further because the *LARS* includes at most $\min\{n, p\} = n = 300$ variables and with $T = 150$, we can expect that, on average, also 150 null variables plus the 5 active variables are included.

5. See the default parameters in the R package implementing the *fixed-X* method and the *model-X* method, which is available at <https://CRAN.R-project.org/package=knockoff> (last access: September 23, 2021).

chosen such that the signal-to-noise ratio (SNR), which is given by $\text{Var}[\mathbf{X}\boldsymbol{\beta}] / \sigma^2$, is equal to one.⁶ The specific values of n , p , p_1 (i.e., the number of active variables), v , T , L , K , SNR, and MC (i.e., the number of Monte Carlo realizations that the results are averaged over) are reported along with the discussion of the results in Figures 3, 4, and 5.

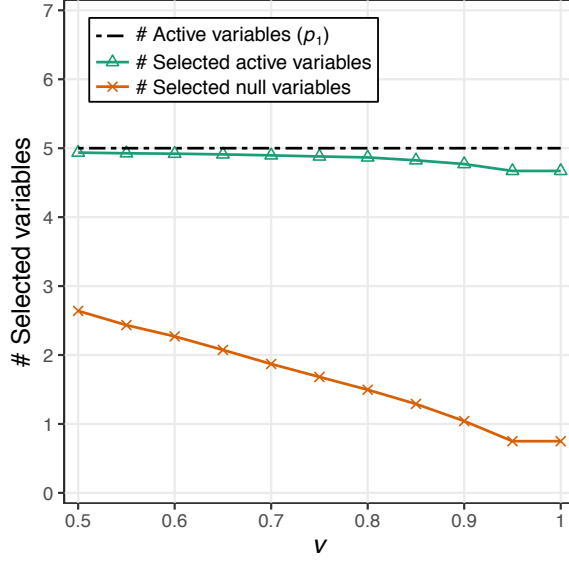


Figure 5: **Ingredient 3** - fusing the candidate sets based on their relative occurrences and a voting level $v \in [0.5, 1)$. The number of selected active variables remains high when increasing the voting level, while the number of selected null variables decreases faster with increasing v . Setup: $n = 150$, $p = 300$, $p_1 = 5$, $T = 3$, $L = p$, $K = 20$, SNR = 1, $MC = 500$.

2.3 Problem Statement

In this section, an optimization problem formalizing the task of selecting as many true positives as possible while controlling the FDR at the target level is formulated. We start with some remarks on notation followed by definitions of the FDR and the TPR, which particularize the generic definitions in (1) for the *T-Knock* filter. For better readability, from now on, the arguments T and L of the estimator of the active set are dropped, i.e., $\hat{\mathcal{A}}(v) := \hat{\mathcal{A}}_L(v, T)$, except when referring specifically to the set in (4) for which the values v^* and T^* result from the calibration that will be discussed in Section 3. Note that the term “included candidates” refers to the variables that were picked (and not dropped) along the solution path of each random experiment while the term “selected variables” refers to the variables whose relative occurrences exceed the voting level $v \in [0.5, 1)$. An overview of frequently used expressions throughout this paper and their meanings is provided in Table 1.

Definition 2 ($V_{T,L}(v)$, $S_{T,L}(v)$ and $R_{T,L}(v)$). *The number of selected null variables $V_{T,L}(v)$, the number of selected active variables $S_{T,L}(v)$, and the number of selected variables $R_{T,L}(v)$ are defined by*

$$\begin{aligned} V_{T,L}(v) &:= |\hat{\mathcal{A}}^0(v)|, \\ S_{T,L}(v) &:= |\hat{\mathcal{A}}^1(v)|, \text{ and} \\ R_{T,L}(v) &:= V_{T,L}(v) + S_{T,L}(v) = |\hat{\mathcal{A}}(v)|, \end{aligned}$$

6. Note that, in this case, Var denotes the sample variance operator.

respectively.

The FDR and TPR expressions in (1) are rewritten using Definition 2 as follows:

Definition 3 (FDP and FDR). *The false discovery proportion (FDP) is defined by*

$$\text{FDP}(v, T, L) := \frac{V_{T,L}(v)}{R_{T,L}(v) \vee 1}$$

and the FDR is defined by

$$\text{FDR}(v, T, L) := \mathbb{E}[\text{FDP}(v, T, L)],$$

where the expectation is taken with respect to the noise in (2).

Definition 4 (TPP and TPR). *The true positive proportion (TPP) is defined by*

$$\text{TPP}(v, T, L) := \frac{S_{T,L}(v)}{p_1 \vee 1}$$

and the TPR is defined by

$$\text{TPR}(v, T, L) := \mathbb{E}[\text{TPP}(v, T, L)],$$

where the expectation is taken with respect to the noise in (2).

Remark 1. *Note that if $R_{T,L}(v)$ is equal to zero, then $V_{T,L}(v)$ is zero, as well. In this case, the denominator in the expression for the FDP is set to one and, thus, the FDP becomes zero. This is a reasonable solution to the “0/0” case, because when no variables are selected there exist no false discoveries. Similarly, when there exist no active variables among the candidates, i.e. $p_1 = S_{T,L}(v) = 0$, the TPP of any selection procedure is equal to zero.*

A major result of this work will be to determine T^* and v^* , such that, for any fixed $L \in \mathbb{N}_+$, the T -Knock filter exhibits the property of maximizing $\text{TPR}(v, T, L)$ while provably controlling $\text{FDR}(v, T, L)$ at any given target level $\alpha \in [0, 1]$. In practice, this amounts to finding the solution of the optimization problem

$$\max_{v, T} \text{TPP}(v, T, L) \quad \text{s.t.} \quad \text{FDP}(v, T, L) \leq \alpha, \quad (5)$$

which is equivalent to

$$\max_{v, T} S_{T,L}(v) \quad \text{s.t.} \quad \text{FDP}(v, T, L) \leq \alpha \quad (6)$$

because p_1 is a constant. However, since we cannot observe $V_{T,L}(v)$ or $S_{T,L}(v)$, we tighten the optimization problem by first replacing $\text{FDP}(v, T, L)$ by a conservative estimator $\widehat{\text{FDP}}(v, T, L)$, for which it holds that $\text{FDR}(v, T, L) = \mathbb{E}[\text{FDP}(v, T, L)] \leq \mathbb{E}[\widehat{\text{FDP}}(v, T, L)] = \widehat{\text{FDR}}(v, T, L)$. The details of the conservative FDP estimator are discussed in Section 3. Then, $S_{T,L}(v)$ is replaced by $R_{T,L}(v)$, which is a conservative choice since $R_{T,L}(v) = S_{T,L}(v) + V_{T,L}(v)$. This results in the following tightened optimization problem:

$$\max_{v, T} R_{T,L}(v) \quad \text{s.t.} \quad \widehat{\text{FDP}}(v, T, L) \leq \alpha. \quad (7)$$

In words: *The number of selected variables is maximized while controlling a conservative estimator of the FDP at the target level α .* Loosely speaking, when controlling $\widehat{\text{FDR}}(v, T, L)$ at a low level and maximizing $R_{T,L}(v)$, large values of $V_{T,L}(v)$ are penalized while favoring large values of $S_{T,L}(v)$.

In the next section, it is shown that the T -Knock filter efficiently solves the tightened optimization problem in (7) and that any solution of the tightened problem is a feasible solution of the original problems in (5) and (6).

Expression	Meaning
$K \in \mathbb{N}_+ \setminus \{1\}$	Number of random experiments.
$L \in \mathbb{N}_+$	Number of knockoffs.
$T \in \{1, \dots, L\}$	Number of included knockoffs after which the forward variable selection process in each random experiment is terminated.
T^*	Optimal value of T as determined by the calibration process.
$v \in [0.5, 1)$	Voting level.
v^*	Optimal value of v as determined by the calibration process.
$\alpha \in [0, 1]$	Target FDR level.
$\mathcal{Z} := \{\text{null } j : j \in \{1, \dots, p\}\}$	Index set of null variables.
$\mathcal{A} := \{\text{active } j : j \in \{1, \dots, p\}\}$	Index set of active variables.
$p_0 := \mathcal{Z} $	Number of null variables.
$p_1 := \mathcal{A} $	Number of (true) active variables.
$p = p_0 + p_1$	Total number of variables.
n	Number of data points.
$\widehat{\mathcal{A}}(v) := \widehat{\mathcal{A}}_L(v, T)$	Estimator of the active set, i.e., index set of the selected variables.
$\widehat{\mathcal{A}}^0(v) := \{\text{null } j : \Phi_{T,L}(j) > v\}$	Index set of the selected null variables.
$\widehat{\mathcal{A}}^1(v) := \{\text{active } j : \Phi_{T,L}(j) > v\}$	Index set of the selected active variables.
$\mathcal{C}_{k,L}(T)$	Candidate set of the k th random experiment, i.e., index set of the included variables in the k th random experiment.

Table 1: Overview of frequently used expressions.

3. Main Results

The main results regarding the properties of the *T-Knock* filter are presented in this section. First, two mild general assumptions are introduced and verified. Then, the FDR control property of the *T-Knock* filter and the main result regarding the knockoff generation process are stated in Theorem 1 and Theorem 2, respectively. Finally, the *T-Knock* calibration algorithm is presented and its feasibility and optimality properties regarding the optimization problems in (5), (6), and (7) are stated in Theorem 3.

3.1 General Assumptions

Since the coefficients of the null variables in the linear model are zero, there is no statistical dependence between the null variables and the response variable. This motivates the assumption that also the number of included null variables in each random experiment is independent of the response variable and, therefore, independent of the noise in the linear model in (2). A consequence of this assumption is that the number of included null variables in each random experiment is independent and identically distributed (i.i.d.) and follows the negative hypergeometric distribution.

Assumption 1. *The number of included null variables in each step t of all random experiments is independent of the response variable.*

Remark 2. *From Assumption 1 it follows that the number of included null variables in a random experiment can be described by a process that randomly picks null variables one at a time without replacement until the process is terminated after T knockoffs are included. Since the included active variables in that process do not count towards the number of included null variables, the total number of candidate variables in the process is p_0 instead of p . The described process can be modeled by the negative hypergeometric distribution.*

Corollary 1. *The numbers of included null variables at step t of all random experiments are i.i.d. random variables following the negative hypergeometric distribution, i.e.,*

$$\sum_{j \in \mathcal{Z}} \mathbb{1}_k(j, t, L) \sim \text{NHG}(p_0 + L, p_0, t), \quad t = 1, \dots, T, k = 1, \dots, K,$$

where \mathcal{Z} is the index set of the null variables.

A numerical verification of Corollary 1, which also implicitly supports Assumption 1, is deferred to Appendix A.

Remark 3. *The negative hypergeometric distribution $\text{NHG}(p_0 + L, p_0, T)$ has three parameters: the total number of elements ($p_0 + L$, i.e., the number of null variables and knockoffs), the number of success elements (i.e., p_0), and the number of included failures after which the experiment is stopped (i.e., T). Thus, it models the number of included null variables before stopping the forward selection process after T knockoffs are included. The expected value of a random variable following the negative hypergeometric distribution with the above specified parameters is given by $T \cdot p_0 / (L + 1)$.*

As shown in the diagram in Figure 1, the estimator of the active set $\widehat{\mathcal{A}}(v)$ results from fusing the candidate sets $\mathcal{C}_{1,L}(T), \dots, \mathcal{C}_{K,L}(T)$ based on a voting level that is applied to the relative occurrences of the candidate variables. Therefore, clearly, the number of selected null variables $V_{T,L}(v)$ is related to the distribution of the number of included null variables in the terminal step $t = T$. We state this relationship as an assumption, since a formal proof that the relationship holds exactly has not yet been established and is subject to ongoing work.

Assumption 2. *For any $v \in [0.5, 1)$, the number of selected null variables is stochastically dominated by a random variable following the negative hypergeometric distribution with parameters specified in Remark 3, i.e.,*

$$V_{T,L}(v) \stackrel{d}{\leq} \text{NHG}(p_0 + L, p_0, T).$$

A numerical verification of Assumption 2 is deferred to Appendix A.

3.2 FDR Control

In Definition 1, the relative occurrence $\Phi_{T,L}(j)$ of the j th candidate variable has been introduced. It can be decomposed into the changes in relative occurrence, i.e.,

$$\Phi_{T,L}(j) = \sum_{t=1}^T \Delta \Phi_{t,L}(j), \quad j = 1, \dots, p,$$

where $\Delta\Phi_{t,L}(j) := \Phi_{t,L}(j) - \Phi_{t-1,L}(j)$ is the change in relative occurrence from step $t - 1$ to t for variable j .⁷ Since the active and the null variables are interspersed in the solution paths of the random experiments, some null variables might appear earlier on the solution paths than some active variables.⁸ Therefore, it is unavoidable that the $\Delta\Phi_{t,L}(j)$'s of the null variables are inflated along the solution paths of the random experiments. Moreover, we observe in our simulations that not only active and null variables but also knockoffs are interspersed in the solution paths of the random experiments. Such a behavior is expected since knockoffs are not related to the response and, therefore, can be interpreted as flagged null variables.

The above considerations motivate the definition of the deflated relative occurrence that is tailored to harnessing the knowledge about the fraction of included knockoffs in each step along the solution paths of the random experiments in order to deflate the $\Delta\Phi_{t,L}(j)$'s of the null variables and, thus, account for the interspersion effect.

Definition 5 (Deflated relative occurrence). *The deflated relative occurrence of variable j is defined by*

$$\Phi'_{T,L}(j) := \sum_{t=1}^T \left(1 - \frac{p - \sum_{q=1}^p \Phi_{t,L}(q)}{L - (t-1)} \cdot \frac{1}{\sum_{q \in \hat{\mathcal{A}}(0.5)} \Delta\Phi_{t,L}(q)} \right) \cdot \Delta\Phi_{t,L}(j), \quad j = 1, \dots, p.$$

In words: *The deflated relative occurrence is the sum over the deflated $\Delta\Phi_{t,L}(j)$'s from step $t = 1$ until step $t = T$. In order to provide an intuitive understanding of the deflated relative occurrence, we rewrite the expression as follows:*

$$\begin{aligned} \Phi'_{T,L}(j) &= \sum_{t=1}^T \left(1 - \frac{\frac{1}{L - (t-1)}}{\frac{\sum_{q \in \hat{\mathcal{A}}(0.5)} \Delta\Phi_{t,L}(q)}{p - \sum_{q=1}^p \Phi_{t,L}(q)}} \right) \cdot \Delta\Phi_{t,L}(j) \\ &= \sum_{t=1}^T \left(1 - \frac{\overbrace{\frac{t - (t-1)}{L - (t-1)}}^{(i)}}{\underbrace{\frac{\frac{1}{K} \sum_{k=1}^K \left(\sum_{q \in \hat{\mathcal{A}}(0.5)} \mathbb{1}_k(q, t, L) - \sum_{q \in \hat{\mathcal{A}}(0.5)} \mathbb{1}_k(q, t-1, L) \right)}{p - \frac{1}{K} \sum_{k=1}^K \sum_{q=1}^p \mathbb{1}_k(q, t, L)}}_{(ii)}}} \right) \cdot \Delta\Phi_{t,L}(j). \end{aligned}$$

The second line follows by rewriting the expression in the denominator within the first line using Definition 1. In the second line, each element of the sum consists of $\Delta\Phi_{t,L}(j)$ multiplied with what we call the *deflation factor*. That factor is computed by subtracting from one the fraction of

7. When using a forward selection method within the *T-Knock* filter that does not drop variables along the solution path (e.g. *LARS*), all $\Phi_{t,L}(j)$'s are non-decreasing in t and, therefore, $\Delta\Phi_{t,L}(j) \geq 0$ for all j . In contrast, when using forward selection methods that might drop variables along the solution path (e.g. *Lasso*), the $\Phi_{t,L}(j)$'s might decrease in t and, therefore, the $\Delta\Phi_{t,L}(j)$'s can be negative. Nevertheless, the relative occurrence $\Phi_{T,L}(j)$ is non-negative for all j and any forward selection method.

8. Many researchers have observed that active and null variables are interspersed in solution paths obtained from sparsity inducing methods, such as the *LARS* algorithm or the *Lasso* (Su et al., 2017; Barber and Candès, 2015).

- (i) the number of included knockoffs at step t , which is always one, divided by the number of non-included knockoffs up until step $t - 1$ and
- (ii) the average number of included candidates at step t divided by the average number of non-included candidates up until step t .

That is, the larger (smaller) the fraction of included candidates at step t compared to the fraction of included knockoffs at step t , the more (less) weight is given to the change in relative occurrence in that step. Loosely speaking, if the number of non-included null variables and knockoffs is equal in step $t - 1$ of the k th random experiment, then allowing one more knockoff to enter the solution path leads, on average, to the inclusion of one more null variable. Thus, if going from step $t - 1$ to t leads to the inclusion of many variables, then still only one null variable is expected to be among them and, therefore, the deflation factor for that step is close to one.

Remark 4. *The reader might wonder whether the deflation factors affect not only the inflated $\Delta\Phi_{t,L}(j)$'s of the null variables but also those of the active variables. Instead of only pointing to the technical details in the appendix, we try to give an intuitive explanation of why the deflation factors have only a negligible effect on the $\Delta\Phi_{t,L}(j)$'s of the active variables: Since usually most active variables enter the solution paths early, i.e., at low values of t and because they are accompanied by very few null variables, the deflation factor is close to one. For this reason, the $\Delta\Phi_{t,L}(j)$'s of the active variables are relatively unaffected. With increasing values of t , the $\Delta\Phi_{t,L}(j)$'s of the active variables are close to zero, because for active variables the increases in relative occurrence are usually high for low values of t and, consequently, low (or even zero) at higher values of t . Summarizing, the deflation factors have little or no effect on the $\Delta\Phi_{t,L}(j)$'s of the active variables because for low values of t they are close to one and for large values of t the $\Delta\Phi_{t,L}(j)$'s of the active variables are close to zero or zero.*

Using the deflated relative occurrences, the estimator of $V_{T,L}(v)$, i.e., the number of selected null variables (see Definition 2), and the corresponding FDP estimator are defined as follows:

Definition 6 (FDP estimator). *The estimator of $V_{T,L}(v)$ is defined by*

$$\widehat{V}_{T,L}(v) := \sum_{j \in \widehat{\mathcal{A}}(v)} (1 - \Phi'_{T,L}(j))$$

and the corresponding estimator of $\text{FDP}(v, T, L)$ is defined by

$$\widehat{\text{FDP}}(v, T, L) = \frac{\widehat{V}_{T,L}(v)}{R_{T,L}(v) \vee 1} \tag{8}$$

with

$$\widehat{\text{FDR}}(v, T, L) := \mathbb{E}[\widehat{\text{FDP}}(v, T, L)]$$

being its expected value.

The main idea behind FDR control for the T -Knock filter is that controlling $\widehat{\text{FDP}}(v, T, L)$ at the target level $\alpha \in [0, 1]$ guarantees that $\widehat{\text{FDR}}(v, T, L)$ is controlled at the target level, as well. In order to achieve this, we define $v \in [0.5, 1)$ as the voting level at which $\widehat{\text{FDP}}(v, T, L)$ is controlled at the target level. Note that the voting level has to be at least 50% to ensure that all selected variables occur in the majority of the candidate sets within the T -Knock filter.

Definition 7 (Voting level). Let $T \in \{1, \dots, L\}$ and $L \in \mathbb{N}_+$ be fixed. Then, the voting level is defined by

$$v := \inf\{\nu \in [0.5, 1) : \widehat{\text{FDP}}(\nu, T, L) \leq \alpha\} \quad (9)$$

with the convention that $v = 1$ if the infimum does not exist.⁹

Remark 5. Recall that our goal, as stated in the optimization problem in (7), is to select as many variables as possible while controlling $\widehat{\text{FDP}}(v, T, L)$ at the target level. For fixed T and L , that goal is achieved by the smallest voting level that satisfies the constraint on $\widehat{\text{FDP}}(v, T, L)$. We can easily see that for any fixed T and L , the voting level in (9) solves the optimization problem in (7). The reason is that for any two voting levels $v_1, v_2 \in [0.5, 1)$ with $v_2 \geq v_1$ satisfying the $\widehat{\text{FDP}}$ constraint in (9), it holds that $R_{T,L}(v_1) \geq R_{T,L}(v_2)$.

Remark 6. If v satisfies Equation (9), then the FDP from Definition 3 can be upper-bounded as follows:

$$\begin{aligned} \text{FDP}(v, T, L) &= \frac{V_{T,L}(v)}{R_{T,L}(v) \vee 1} \\ &= \frac{\widehat{V}_{T,L}(v)}{R_{T,L}(v) \vee 1} \cdot \frac{V_{T,L}(v)}{\widehat{V}_{T,L}(v)} \\ &= \widehat{\text{FDP}}(v, T, L) \cdot \frac{V_{T,L}(v)}{\widehat{V}_{T,L}(v)} \\ &\leq \alpha \cdot \frac{V_{T,L}(v)}{\widehat{V}_{T,L}(v)} \\ &\leq \alpha \cdot \frac{V_{T,L}(v)}{\widehat{V}'_{T,L}(v)}, \end{aligned}$$

where $\widehat{V}'_{T,L}(v)$ is defined by

$$\widehat{V}'_{T,L}(v) := \widehat{V}_{T,L}(v) - \sum_{j \in \widehat{\mathcal{A}}(v)} (1 - \Phi_{T,L}(j)).$$

Before the FDR control theorem is formulated, we introduce a very mild but necessary assumption:

Assumption 3. For sufficiently large $T \in \{1, \dots, L\}$ it holds that

$$\widehat{V}'_{T,L}(v) \approx \sum_{t=1}^T \frac{p_0 - \sum_{q \in \mathcal{Z}} \Phi_{t,L}(q)}{L - (t-1)} \cdot \frac{\sum_{j \in \widehat{\mathcal{A}}^0(v)} \Delta \Phi_{t,L}(j)}{\sum_{q \in \widehat{\mathcal{A}}^0(0.5)} \Delta \Phi_{t,L}(q)}.$$

In order not to disturb the reading flow, the motivation and technical details behind Assumption 3 and its numerical verification are deferred to Appendix A.

9. The voting level can be interpreted as a stopping time. The term 'stopping time' stems from martingale theory (Williams, 1991). In the proof of Lemma 1, it is shown that indeed v is a stopping time with respect to some still to be defined filtration of a still to be defined stochastic process (see Appendix B). Note that the convention of setting $v = 1$ if the infimum does not exist ensures that no variables are selected when there exists no triple (T, L, v) that satisfies Equation (9).

Theorem 1 (FDR control). *Suppose that Assumptions 1, 2, and 3 are fulfilled. Then, for all triples $(T, L, v) \in \{1, \dots, L\} \times \mathbb{N}_+ \times [0.5, 1)$ that satisfy Equation (9) and as $K \rightarrow \infty$, the T -Knock filter controls the FDR at any fixed target level $\alpha \in [0, 1]$, i.e.,*

$$\text{FDR}(v, T, L) = \mathbb{E}[\text{FDP}(v, T, L)] \leq \alpha.$$

Proof sketch. Using the upper bound of the FDP from Remark 6, the FDR can be upper-bounded as follows:

$$\begin{aligned} \text{FDR}(v, T, L) &= \mathbb{E}[\text{FDP}(v, T, L)] \\ &\leq \alpha \cdot \mathbb{E}\left[\frac{V_{T,L}(v)}{\widehat{V}'_{T,L}(v)}\right]. \end{aligned}$$

What remains to be shown is that $\mathbb{E}[V_{T,L}(v) / \widehat{V}'_{T,L}(v)] \leq 1$. Let $H_{T,L}(v) := V_{T,L}(v) / \widehat{V}'_{T,L}(v)$ be a random variable, v be as given in Definition 7, and $\mathcal{F}_v := \sigma(\{V_{T,L}(u)\}_{u \geq v}, \{\widehat{V}'_{T,L}(u)\}_{u \geq v})$ be a backward-filtration with respect to v . First, it is shown that the discrete stochastic process $\{H_{T,L}(v)\}_{v \in \mathcal{V}}$ with index set $\mathcal{V} := \{\Phi_{T,L}(j) : \Phi_{T,L}(j) > 0.5, j = 1, \dots, p\}$ is a discrete backward-running super-martingale with respect to \mathcal{F}_v . Then, and since the voting level v is a stopping time that is adapted to \mathcal{F}_v , Doob's optional stopping theorem is applied to obtain an upper-bound on the expectation of $H_{T,L}(v)$, which yields $\mathbb{E}[H_{T,L}(v)] \leq \mathbb{E}[H_{T,L}(0.5)]$. Finally, it is shown that $\mathbb{E}[H_{T,L}(0.5)] \leq 1$ and the theorem follows. \square

For ease of readability, only a brief proof sketch has been presented at this point and the technical details are deferred to Appendix B.

3.3 Knockoff Generation

As shown in Figure 1, the T -Knock filter generates L i.i.d. knockoffs for each random experiment by sampling each element of the knockoff vectors from the standard normal distribution, i.e.,

$$\mathring{\mathbf{x}}_l = [\mathring{\mathbf{x}}_{1,l}, \dots, \mathring{\mathbf{x}}_{n,l}]^\top, \text{ where } \mathring{\mathbf{x}}_{i,l} \sim \mathcal{N}(0, 1), i = 1, \dots, n, l = 1, \dots, L.$$

This raises the question whether knockoffs can be sampled from other distributions, as well, to serve as flagged null variables. From an asymptotic point of view, i.e., $n \rightarrow \infty$, and if some mild conditions hold, the answer to this question is that knockoffs can be sampled from any probability distribution in order to serve as flagged null variables within the T -Knock filter. In the following, we will prove the validity of this statement for any forward selection procedure that uses sample correlations of the predictors with the response or with the current residuals in each forward selection step to determine which variable is included in the respective step. Thus, the statement holds for the *LARS* algorithm and related methods (e.g., *Lasso*, *adaptive Lasso*, and *elastic net*).

Recall that null variables and knockoffs are not related to the response. For null variables the independence holds by definition and for knockoffs it holds because knockoffs are generated without using any information about the response.¹⁰ Therefore, in each step t along the solution path of

10. Note that the knockoff generation processes of the *fixed-X* and the *model-X* method, i.e., the benchmark methods, is different to our approach. Although these methods also do not use any information about the response to generate the knockoffs, unlike the proposed T -Knock filter, their knockoff generation processes must incorporate the covariance structure of the predictor matrix, which leads to a large computation time, especially for high dimensions (see Figures 3 and 7).

any random experiment, the probability of including a knockoff is higher than the probability of including a null variable if the number of non-included knockoff variables up until step $t - 1$ is larger than the number of non-included null variables up until step $t - 1$ and vice versa. These considerations suggest that only the number of knockoffs within the enlarged predictor matrices is relevant for the behavior of the forward selection process in each random experiment. That is, for $n \rightarrow \infty$, the distribution from which the knockoffs are sampled has no influence on the distribution of the correlation variables

$$\mathring{G}_{l,m,k} := \sum_{i=1}^n \gamma_{i,m,k} \cdot \mathring{X}_{i,l,k}, \quad l \in \mathcal{K}_{m,k}, \quad m \geq 1, \quad k = 1, \dots, K,$$

where $\gamma_{i,m,k}$ is the i th element of $\boldsymbol{\gamma}_{m,k} := \mathbf{y} - \mathbf{X}\hat{\boldsymbol{\beta}}_{m,k}$, namely the residual vector in the m th forward selection step of the k th random experiment with $\hat{\boldsymbol{\beta}}_{m,k}$ and $\mathcal{K}_{m,k}$ being the estimate of the parameter vector and the index set of the non-included knockoffs in the m th forward selection step of the k th random experiment, respectively. Note that $\boldsymbol{\gamma}_{1,k} = \mathbf{y}$ for all k , since $\hat{\boldsymbol{\beta}}_{1,k} = \mathbf{0}$ for all k , i.e., the residual vector in the first step of the forward selection process is simply the response vector \mathbf{y} . The random variable $\mathring{X}_{i,l,k}$ represents the i th element of the l th knockoff within the k th random experiment. Summarizing, $\mathring{G}_{l,m,k}$ can be interpreted as the weighted sum of the i.i.d. random variables $\mathring{X}_{1,l,k}, \dots, \mathring{X}_{n,l,k}$ with fixed weights $\gamma_{1,m,k}, \dots, \gamma_{n,m,k}$. With these preliminaries in place, the second main theorem is formulated as follows:

Theorem 2 (Knockoff generation). *Let $\mathring{X}_{i,l,k}$, $i = 1, \dots, n$, $l \in \mathcal{K}_{m,k}$, $m \geq 1$, $k = 1, \dots, K$, be standardized i.i.d. knockoff random variables (i.e., $\mathbb{E}[\mathring{X}_{i,l,k}] = 0$ and $\text{Var}[\mathring{X}_{i,l,k}] = 1$ for all i, l, m, k) following any probability distribution. Define*

$$D_{n,l,m,k} := \frac{1}{\Gamma_{n,m,k}} \cdot \mathring{G}_{l,m,k},$$

where $\Gamma_{n,m,k}^2 := \sum_{i=1}^n \gamma_{i,m,k}^2$ with $\Gamma_{n,m,k} > 0$ for all n, m, k and with fixed $\gamma_{i,m,k} \in \mathbb{R}$ for all i, m, k . Suppose that

$$\lim_{n \rightarrow \infty} \frac{\gamma_{i,m,k}}{\Gamma_{n,m,k}} = 0, \quad i = 1, \dots, n,$$

for all n, m, k . Then, as $n \rightarrow \infty$,

$$D_{n,l,m,k} \xrightarrow{d} D, \quad D \sim \mathcal{N}(0, 1),$$

for all l, m, k .

Proof sketch. The Lindeberg-Feller central limit theorem is applicable because $\mathring{X}_{i,l,k}$, $i = 1, \dots, n$, $l \in \mathcal{K}_{m,k}$, $m \geq 1$, $k = 1, \dots, K$, are i.i.d random variables for which it holds that $\mathbb{E}[D_{n,l,m,k}] = 0$ and $\text{Var}[D_{n,l,m,k}] = 1$. Moreover, since $\mathring{Q}_{i,l,m,k} := \gamma_{i,m,k} \cdot \mathring{X}_{i,l,k} / \Gamma_{n,m,k}$ satisfies the Lindeberg condition for all l, m, k , the theorem follows. \square

The details of the proof are deferred to Appendix B.

Remark 7. *Loosely speaking, Theorem 2 states that regardless of the distribution from which the knockoffs are sampled, the correlation variables follow the standard normal distribution as $n \rightarrow \infty$. That is, the distribution of the knockoffs has no influence on the resulting distribution of the correlation variables. Note that in the LARS algorithm, the correlations of the predictors with the*

residual vectors along the solution path determine which variable enters the solution path in the respective step. So, we can conclude that the decisions of which variable enters next along the solution path is independent of the distribution of the knockoffs. Thus, the knockoffs can be sampled from any distribution to serve as flagged null variables within the T -Knock filter.

Remark 8. Note that our knockoffs serve as flagged null variables within multiple random experiments of the proposed T -Knock filter, while the knockoffs for the fixed- X method (Barber and Candès, 2015) and model- X method (Candès et al., 2018) are specifically designed to act as counterparts of the original variables in only one single run of the underlying variable selection method (see Section 4.1.2 for more details). Further, note that sampling knockoffs from any probability distribution to serve as flagged null variables is only reasonable in combination with multiple random experiments as conducted by the proposed T -Knock filter. We emphasize that Theorem 2 is not stating that fixed- X and model- X knockoffs can be sampled from any probability distribution.

3.4 The T -Knock Filter: Calibration Algorithm

This section describes the proposed T -Knock calibration algorithm, which efficiently solves the optimization problem in (7) and provides feasible solutions for (5) and (6). The pseudocode of the T -Knock calibration method is provided in the following algorithm:

Algorithm 1 (T -Knock Calibration).

1. **Input:** $\alpha \in [0, 1]$, K , L , \mathbf{X} , \mathbf{y} .
2. **Set** $T = 1$, $\widehat{\text{FDP}}(v = 1, T, L) = 0$, $\Delta v = \frac{1}{K}$.
3. **While** $\widehat{\text{FDP}}(v = 1, T, L) \leq \alpha$ and $T \leq L$ **do**
 - 3.1. **For** $v = 0.5, 0.5 + \Delta v, 0.5 + 2 \cdot \Delta v, \dots, 1 - \Delta v$ **do**
 - i. **Compute** $\widehat{\text{FDP}}(v, T, L)$ as in (8).
 - ii. **If** $\widehat{\text{FDP}}(v, T, L) \leq \alpha$

Compute $\widehat{\mathcal{A}}_L(v, T)$ as in (4).

Else

Set $\widehat{\mathcal{A}}_L(v, T) = \emptyset$.
 - 3.2. **Set** $T \leftarrow T + 1$.
4. **Solve**

$$\max_{v', T'} |\widehat{\mathcal{A}}_L(v', T')| \quad \text{s.t.} \quad T' \in \{1, \dots, T - 1\}$$

$$v' \in \{0.5, 0.5 + \Delta v, 0.5 + 2 \cdot \Delta v, \dots, 1 - \Delta v\}$$

and let (v^*, T^*) be a solution.

5. **Output:** (v^*, T^*) and $\widehat{\mathcal{A}}_L(v^*, T^*)$.

Remark 9. In case of multiple solutions, we recommend to choose the solution with the largest v . The reason is that such a solution provides the variables that were selected most frequently. Nevertheless, all solutions to the calibration problem that are computed using Algorithm 1 provide FDR control at the target level while maximizing the number of selected variables.

The algorithm flow is as follows: First the number of knockoffs L and the number of random experiments K are set (usually $L = p$ and $K = 20$).¹¹ Then, setting $v = 1$ and starting at $T = 1$, the number of included knockoffs is iteratively increased until reaching the value of T for which the FDP estimate at a voting level of 100% exceeds the target level for the first time. In each iteration, before the target level is reached, $\widehat{\mathcal{A}}_L(v, T)$ is computed as in (4) on a grid for v , while for values of v for which $\widehat{\text{FDP}}(v, T, L)$ exceeds the target level $\widehat{\mathcal{A}}_L(v, T)$ is equal to the empty set.

The reason for exiting the loop in Step 3, i.e., when the FDP estimate at a voting level of 100% exceeds the target level for the first time, is based on two key observations from our still to be presented simulation results:

1. For any fixed T and L the lowest average value of $\widehat{\text{FDP}}(v, T, L)$ is attained at a voting level of 100%.
2. For any fixed v and L the average value of $\widehat{\text{FDP}}(v, T, L)$ increases as T increases.

A mathematical proof of these observations has not yet been established and is subject to ongoing work. Therefore, we state them in the following assumption and give a numerical verification in Figure 6:

Assumption 4. *Let K and L be fixed. Then, for any fixed T , $\widehat{\text{FDP}}(v, T, L)$ is monotonically decreasing with respect to v and, for any fixed v , $\widehat{\text{FDP}}(v, T, L)$ is monotonically increasing with respect to T .*

So, with Assumption 4 there exist no v and L for any $T \geq T_{\max}$ such that $\widehat{\text{FDP}}(v, T, L) \leq \alpha$. This leads to the third main theorem of this paper.

Theorem 3 (Optimality of Algorithm 1). *Let (v^*, T^*) be a solution determined by Algorithm 1 and suppose that Assumption 4 holds. Then, (v^*, T^*) is an optimal solution of (7) and a feasible solution of (5) and (6).*

Proof sketch. Since the objective functions of the optimization problems in Step 4 of Algorithm 1 and in (7) are equivalent, i.e., $|\widehat{\mathcal{A}}_L(v, T)| = R_{T,L}(v)$, it only needs to be shown that the feasible set in Step 4 of the algorithm contains the feasible set of (7). Since the conditions of the optimization problems in (5), (6), and (7) are equivalent, this also proves that (v^*, T^*) is a feasible solution of (5) and (6). \square

The details of the proof are deferred to Appendix B.

3.5 Extension to the Calibration Algorithm

In Theorem 1, we have also stated that the T -Knock filter controls the FDR at the target level for any choice of the number of knockoffs L . However, the choice of L has an influence on how tightly the target FDR level is controlled. Since controlling the FDR more tightly usually increases the TPR (i.e., power), it is desirable to choose the parameters T -Knock filter accordingly. We will see in the simulations in Section 4 that with increasing L , the FDR can be more tightly controlled at low target levels. In order to harness the positive effects that come with larger values of L and to limit the increased memory requirement for high values of L , we propose an extended version of the calibration algorithm that jointly determines v , T , and L such that the FDR is more tightly

11. As already mentioned in Section 2.2, K is not subject to optimization. In practice, choosing $K = 20$ provided excellent results (see Section 4).

controlled at the target FDR level while not running out of memory.¹² The major difference to Algorithm 1 is that the number of knockoffs L is iteratively increased until the estimate of the FDP falls below the target FDR level α . The pseudocode of the extended T -Knock calibration method is provided in the following algorithm:¹³

Algorithm 2 (Extended T -Knock Calibration).

1. **Input:** $\alpha \in [0, 1]$, K , \mathbf{X} , \mathbf{y} , \tilde{v} , L_{\max} , T_{\max} .
2. **Set** $L = p$, $T = 1$, $\widehat{\text{FDP}}(v = \tilde{v}, T, L) = 1$.
3. **While** $\widehat{\text{FDP}}(v = \tilde{v}, T, L) \geq \alpha$ and $L \leq L_{\max}$ **do**:
 - Set** $L \leftarrow L + p$
4. **Set** $\widehat{\text{FDP}}(v = 1, T, L) = 0$, $\Delta v = \frac{1}{K}$.
5. **While** $\widehat{\text{FDP}}(v = 1, T, L) \leq \alpha$ and $T \leq T_{\max}$ **do**
 - 5.1. **For** $v = 0.5, 0.5 + \Delta v, 0.5 + 2 \cdot \Delta v, \dots, 1 - \Delta v$ **do**
 - i. **Compute** $\widehat{\text{FDP}}(v, T, L)$ as in (8).
 - ii. **If** $\widehat{\text{FDP}}(v, T, L) \leq \alpha$
 - Compute** $\widehat{\mathcal{A}}_L(v, T)$ as in (4).
 - Else**
 - Set** $\widehat{\mathcal{A}}_L(v, T) = \emptyset$.
 - 5.2. **Set** $T \leftarrow T + 1$.
6. **Solve**

$$\max_{v', T'} |\widehat{\mathcal{A}}_L(v', T')| \quad \text{s.t.} \quad T' \in \{1, \dots, T - 1\}$$

$$v' \in \{0.5, 0.5 + \Delta v, 0.5 + 2 \cdot \Delta v, \dots, 1 - \Delta v\}$$

and let (v^*, T^*) be a solution.

7. **Output:** (v^*, T^*) and $\widehat{\mathcal{A}}_L(v^*, T^*)$.

Note that the extension to Algorithm 1 lies in Step 2 and Step 3. Additionally, and in contrast to Algorithm 1, the input to the algorithm is extended by a reference voting level $\tilde{v} \in [0.5, 1)$ and the maximum values of L and T , namely L_{\max} and T_{\max} . The algorithm flow is as follows: First L and T are set as follows: $L = p$ and $T = 1$. Then, starting at $L = p$ the number of knockoffs L is

12. The reader might raise the question whether also the computation time increases with increasing L . There is no definite answer to this question. On the one hand, for very large values of L the computation time might increase because the complexity of the T -Knock filter is linear in p . On the other hand, with increasing L , the solution paths of the experiments are terminated earlier because the probability of selecting knockoffs grows with increasing L . Thus, increasing L might increase or decrease the computation depending on whether the first or the second effect dominates.

13. An R package containing the implementation of the T -Knock filter, the calibration algorithm in Algorithm 1, and the extended calibration algorithm in Algorithm 2 will be made available on the GitHub accounts of the authors and will be submitted to CRAN (<https://cran.r-project.org/>).

iteratively increased in steps of p until the estimate of the FDP at the voting level \tilde{v} falls below the target FDR level α or L exceeds L_{\max} . The rest of the algorithm is as in Algorithm 1 except that the loop in Step 4 is exited when T exceeds T_{\max} . What remains to be discussed are the choices of \tilde{v} , L_{\max} , and T_{\max} :

1. $\tilde{v} = 0.75$: The choice of \tilde{v} is a compromise between the 50% and the 100% voting levels. Setting $\tilde{v} = 0.5$ would require low values of L to push $\widehat{\text{FDP}}(v = \tilde{v}, T, L)$ below the target FDR level while setting $\tilde{v} = 1$ would require very high values of L . Thus, $\tilde{v} = 0.75$ is a compromise between tight FDR control and memory consumption.
2. $L_{\max} = 10p$: In order to allow for sufficiently large values of L such that tight FDR control is possible while not running out of memory, setting $L_{\max} = 10p$ has proven to be a practical choice. Note that the FDR control property in Theorem 1 holds for any choice of L . However, we can achieve tighter FDR control with larger values of L .
3. $T_{\max} = \lceil n/2 \rceil$: As discussed in the caption of Figure 3, the *LARS* algorithm includes at most $\min\{n, p\}$ variables and in high-dimensional settings ($p > n$), the maximum number of included variables in each random experiment is n . Since for $L = p$ we expect roughly as many null variables as knockoffs in very sparse settings, choosing $T_{\max} = \lceil n/2 \rceil$ ensures that the *LARS* algorithm could potentially run until (almost) the end of the solution path. In contrast, for $L = 10p$ we expect 10 times as many knockoffs as null variables in very sparse settings. Thus, for $L = p$ we allow the solution paths to potentially run until the end, although this might only happen in rare cases, while for $L = 2p, \dots, 10p$ we restrict the run length. This is a compromise between a higher computation time and a higher TPR (i.e., power) that are both associated with larger values of T_{\max} .

3.6 Computational Complexity

The computational complexities of sampling knockoffs from the univariate standard Gaussian distribution and fusing the candidate sets are negligible compared to the computational complexity of the utilized forward selection method. Therefore, it is sufficient to analyze the computational complexities of the early terminated forward selection processes. We restrict the following analysis to the *LARS* algorithm.¹⁴ The κ th step of the *LARS* algorithm has the complexity $\mathcal{O}((p - \kappa) \cdot n + \kappa^2)$, where the terms $(p - \kappa) \cdot n$ and κ^2 account for the complexity of determining the variable with the highest absolute correlation with the current residual (i.e., the next to be included variable) and the so-called equiangular direction vector, respectively. Replacing p by $p + L$, since the original predictor matrix is replaced by the enlarged predictor matrix, and summing up the complexities of all steps until termination yields the computational complexity of the *T-Knock* filter. First, we define the run lengths as the cardinalities of the respective candidate sets, i.e.,

$$\kappa_{T,L}(k) := |\mathcal{C}_{k,L}(T)|, \quad k = 1, \dots, K,$$

14. Since the *Lasso* solution path can be computed by a slightly modified *LARS* algorithm, the *Lasso* and the *LARS* algorithm have the same computational complexity.

and assume $L \geq p$. Then, the sum over all steps until the termination of the k th random experiment is given by

$$\begin{aligned} \sum_{\kappa=1}^{\kappa_{T,L}(k)} ((p+L-\kappa) \cdot n + \kappa^2) &= n \cdot \kappa_{T,L}(k) \cdot (p+L) - n \cdot \sum_{\kappa=1}^{\kappa_{T,L}(k)} \kappa + \sum_{\kappa=1}^{\kappa_{T,L}(k)} \kappa^2 \\ &\leq n \cdot \kappa_{T,L}(k) \cdot (p+L) + (\kappa_{T,L}(k))^3. \end{aligned}$$

We can write $L = \lceil \eta \cdot p \rceil$, $\eta > 0$, and the expected run length can be upper bounded as follows:

$$\mathbb{E}[\kappa_{T,L}(k)] \leq p_1 + T + \mathbb{E}[\Psi] = p_1 + T + \frac{T}{L+1} \cdot p_0 \leq p_1 + 2T,$$

where the first equation follows from $\Psi \sim \text{NHG}(p_0+L, p_0, T)$ and the second inequality holds because $L \geq p$. So, the expected computational complexity of the proposed T -Knock filter is $\mathcal{O}(np)$. The computational complexity of the original (i.e., non-terminated) $LARS$ algorithm in high-dimensional settings is $\mathcal{O}(p^3)$. Thus, on average the high computational complexity of the $LARS$ algorithm does not carry over to the T -Knock filter because within the T -Knock filter the solution paths of the random experiments are early terminated. Moreover, the computational complexity of the T -Knock filter is the same as that of the pathwise coordinate descent algorithm (Friedman et al., 2010).

4. Numerical Simulations

In this section, the performances of the proposed T -Knock filter and the benchmark methods are compared in a simulation study. First, the benchmark methods are briefly described. Then, the simulation setups are introduced and the results are presented and discussed.

4.1 Benchmark Methods for FDR Control

The benchmark methods in low-dimensional settings (i.e., $p \leq n$) are the Benjamini-Hochberg (BH) method (Benjamini and Hochberg, 1995), the Benjamini-Yekutieli (BY) method (Benjamini and Yekutieli, 2001), and the *fixed-X* methods (Barber and Candès, 2015), while the *model-X* methods (Candès et al., 2018) are the benchmarks in high-dimensional settings (i.e., $p > n$). These methods are briefly described and discussed in the following.

4.1.1 THE BH AND THE BY METHOD

For low-dimensional sparse regression, we can formulate the null hypotheses $H_j : \beta_j = 0$, $j = 1, \dots, p$ with associated p -values P_1, \dots, P_p . Thus, when a variable is selected, we can interpret this as the rejection of the corresponding null hypothesis in favor of the alternative hypothesis. The BH method and the BY method were designed to control the FDR at the target level $\alpha \in [0, 1]$ for multiple hypothesis testing based on p -values. For all variables in the sparse regression setting, the p -values are computed and sorted in an ascending order. Then, the estimate of the number of active variables $\hat{p}_1(\alpha)$ is determined by finding the largest p -value that does not exceed a threshold depending on α by solving

$$\hat{p}_1(\alpha) = \max \left\{ m : P_m \leq \frac{m}{p \cdot c(p)} \cdot \alpha \right\},$$

where $c(p) = 1$ for the BH method and $c(p) = \sum_{j=1}^p 1/j \approx \ln(p) + \gamma$ for the BY method with $\gamma \approx 0.577$ being the Euler-Mascheroni constant. If no such $\hat{p}_1(\alpha)$ exists, then no hypothesis is

rejected. Otherwise, the variables corresponding to the $\hat{p}_1(\alpha)$ smallest p -values are selected. The *BH* method requires independent hypotheses or, at least, a so-called positive regression dependency among the candidates to guarantee FDR control at the target level. In contrast, the *BY* method provably controls the FDR at the target level and does not require independent hypotheses or any assumptions regarding the dependency among the hypotheses. However, the *BY* method is more conservative than the *BH* method, i.e., it achieves a considerably lower power than the *BH* method at the same target FDR level.

4.1.2 THE FIXED-X AND THE MODEL-X METHODS

The *fixed-X* knockoff method is a relatively new method for controlling the FDR in sparse linear regression settings. Since it requires $n \geq 2p$ observations, it is not suitable for high-dimensional settings. The method generates a knockoff matrix $\mathring{\mathbf{X}}$ consisting of p knockoff variables and appends it to the original predictor matrix. Unlike for our proposed *T-Knock* filter, the knockoff variables are designed to mimic the correlation structure of \mathbf{X} . Further, they are designed to be, conditional on the original variables, independent of the response. Hence, the knockoff variables act as a control group and when a knockoff variable enters the active set before its original counterpart it provides some evidence against this variable being a true positive.

The predictor matrix of, e.g., the *Lasso* in (3) is then replaced by $[\mathbf{X} \ \mathring{\mathbf{X}}]$ and the λ -values corresponding to the first entry points of the original and knockoff variables are extracted from the solution path resulting in $Z_j = \sup\{\lambda : \hat{\beta}_j \neq 0 \text{ first time}\}$ and $\mathring{Z}_j = \sup\{\lambda : \hat{\beta}_{j+p} \neq 0 \text{ first time}\}$, $j = 1, \dots, p$. The authors suggest to design the test statistics

$$W_j = (Z_j \vee \mathring{Z}_j) \cdot \text{sign}(Z_j - \mathring{Z}_j), \quad j = 1, \dots, p \quad (10)$$

and to determine the threshold

$$\tau = \min \left\{ \tau' \in \mathcal{W} : \frac{b + |\{j : W_j \leq -\tau'\}|}{|\{j : W_j \geq \tau'\}| \vee 1} \leq \alpha \right\}, \quad (11)$$

where $\mathcal{W} = \{|W_j| : j = 1, \dots, p\} \setminus \{0\}$. Note that this is only one of the test statistics that were proposed by the authors. In general, many other test statistics obeying a certain sufficiency and anti-symmetry property are suitable for the knockoff method. In our simulations, we stick to the test statistic in (10). In (11), $b = 0$ yields the knockoff method and $b = 1$ the more conservative (higher threshold τ) knockoff+ method. Finally, only those variables whose test statistics exceed the threshold are selected, which gives us the selected active set $\hat{\mathcal{A}} = \{j : W_j \geq \tau\}$. The knockoff+ method controls the FDR at the target level α and the knockoff method controls a modified version of the FDR. The advantage of the knockoff over the knockoff+ method is that it is less conservative and will, generally, have a higher power at the cost of controlling only a related quantity but not the FDR.

The *model-X* knockoff method was proposed as an extension to the *fixed-X* knockoff method for high-dimensional settings (Candès et al., 2018). It does not require any knowledge about the conditional distribution of the response given the explanatory variables $Y|X_1, \dots, X_p$ but needs to know the distribution of the covariates (X_{i1}, \dots, X_{ip}) , $i = 1, \dots, n$. The difference to the deterministic design of *fixed-X* knockoffs is that *model-X* knockoffs need to be designed probabilistically by sequentially sampling each knockoff predictor \mathring{X}_j , $j = 1, \dots, p$, from the conditional distribution of $X_j|X_{-j}, \mathring{X}_{1:j-1}$, where X_{-j} is the set of all explanatory variables except for X_j and $\mathring{X}_{1:j-1} := \{\mathring{X}_1, \dots, \mathring{X}_{j-1}\}$. However, the authors state that determining a new conditional distribution for each knockoff predictor and sampling from it turned out to be complicated and

computationally very expensive (Candès et al., 2018). The only case in which *model-X* knockoffs can be easily constructed by sampling from the Gaussian distribution with certain mean vector and covariance matrix is when the covariates follow the Gaussian distribution. For all other distributions of the covariates, especially when p is large, the authors consider an approximate construction of *model-X* knockoffs which yields the so-called second-order *model-X* knockoffs. Unfortunately, however, there is no proof that FDR control is achieved with second-order *model-X* knockoffs. Nevertheless, in our simulations we consider these knockoffs. Moreover, for $p > 500$ we consider the approximate semidefinite program (asdp) instead of the original semidefinite program that needs to be solved to construct second-order *model-X* knockoffs. This is the default choice in the R package accompanying the *fixed-X* and *model-X* papers.¹⁵

4.2 Setup and Results

Similarly to the numerical examples in Section 2.3, we generate a sparse high-dimensional setting with n observations, p predictors, and a response given by the linear model in (2). Further, $\beta_j = 1$ for p_1 randomly selected j 's and $\beta_j = 0$ for the others. The predictors are sampled from the standard normal distribution. The noise level σ is chosen such that the signal-to-noise ratio (SNR), which is given by $\text{Var}[\mathbf{X}\boldsymbol{\beta}] / \sigma^2$, is equal to the desired value. The specific values of the above described generic simulation setting and the parameters of the *T-Knock* filter, i.e., the values of n , p , p_1 , SNR, K , L , T , v , are specified in the figure captions. The results are averaged over 955 Monte Carlo replications.¹⁶ First, and in order to assess the $\widehat{\text{FDR}}$ control performance and the achieved power of the *T-Knock* filter the average FDP, average $\widehat{\text{FDP}}$, and the average TPP are computed over a two-dimensional grid for v and T for different values of L . Then, leaving all other parameters in this setup fixed, we compare the performance of the proposed *T-Knock* filter in combination with the proposed extended calibration algorithm in Algorithm 2 with the benchmark methods for different values of p_1 and the SNR at a target FDR level of 10%. Finally, a sweep over p is conducted to assess the scalability of the *T-Knock* filter and the benchmark methods to high dimensions in terms of computation time.

Note that the reported average FDP, the average $\widehat{\text{FDP}}$, and the average TPP (i.e., averaged over 955 Monte Carlo replications) are estimates of the FDR, the $\widehat{\text{FDR}}$, and the TPR, respectively. For this reason, the results are discussed in terms of the FDR and the TPR in the captions of the figures and subfigures, while the axes labels emphasize that the average FDP and the average TPP are plotted.

The simulation results confirm that the proposed *T-Knock* filter possesses the FDR control property. Moreover, the simulation results show that the *T-Knock* filter outperforms the benchmark methods and that its computation time is multiple orders of magnitude lower than that of its competitors. The detailed descriptions and discussions of the simulation results are given within the captions of Figures 6, 7, and 8.¹⁷

15. The R package implementing the *fixed-X* method and the *model-X* method is available at <https://CRAN.R-project.org/package=knockoff> (last access: September 23, 2021).

16. The reason for running 955 Monte Carlo replications is that the simulations were conducted on the Lichtenberg High Performance Cluster of the Technische Universität Darmstadt, which consists of multiple nodes of 96 CPUs each. In order to run computationally efficient simulations, our computation jobs are designed to request 2 nodes and run 5 cycles on each CPU while one CPU acts as the master, i.e., $(2 \cdot 96 - 1) \cdot 5 = 955$.

17. Additional simulation results that allow for a performance comparison of the proposed *T-Knock* filter to the *BH* method, the *BY* method, and the *fixed-X* knockoff methods in a low-dimensional setting are deferred to Appendix C.

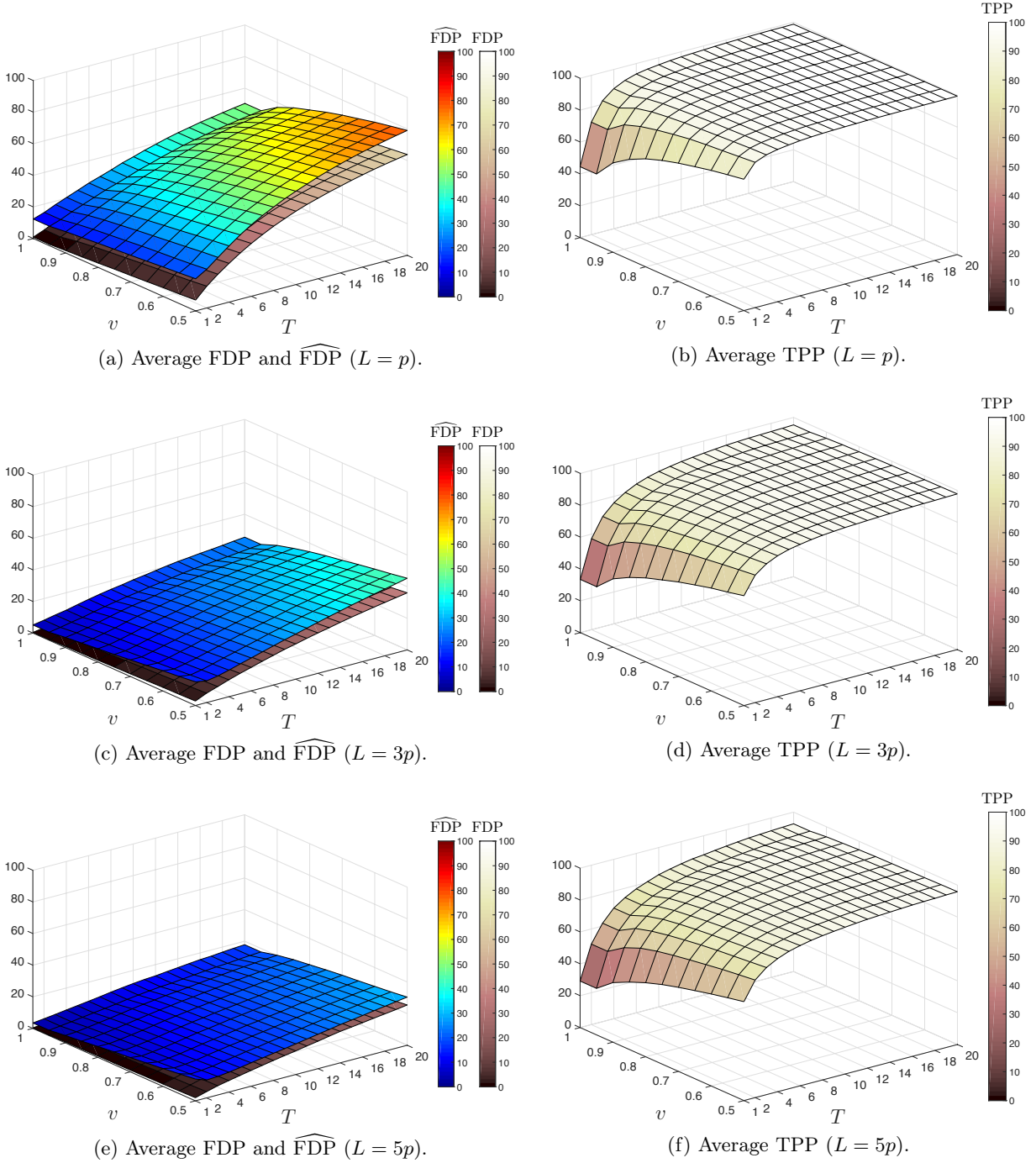


Figure 6: The T -Knock filter controls the FDR for all values of v and T while achieving a high power even at low values of T . Note that the FDR control is tighter for large values of L which has led to the development of the extended calibration algorithm in Section 3.5. Moreover, note that Assumption 4 holds on average, i.e., $\widehat{\text{FDP}}(v, T, L)$ is monotonically decreasing with respect to v and monotonically increasing with respect to T on average. Setup: $n = 300$, $p = 1000$, $p_1 = 10$, $K = 20$, $\text{SNR} = 1$, $MC = 955$.

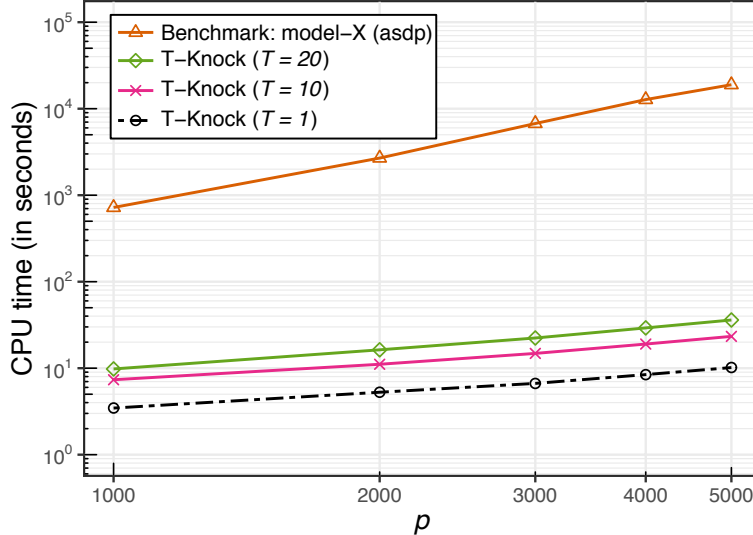


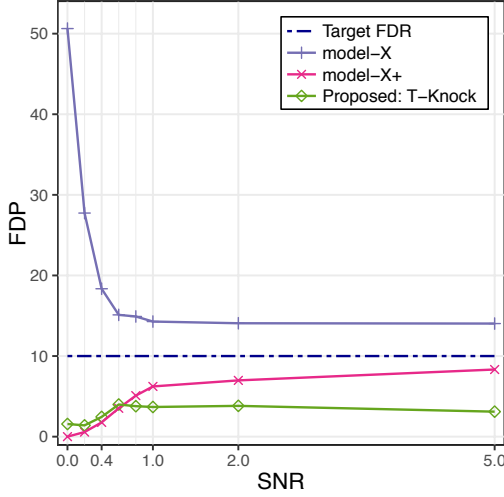
Figure 7: The computation time of the T -Knock filter is multiple orders of magnitude lower than that of the $model$ -X knockoff method. The reference computation time is that of the T -Knock filter with $L = p$. Note that, e.g., for $p = 5000$ the absolute computation of the T -Knock filter for $T = 1$ is only 10 seconds as compared to more than 5 hours for the $model$ -X knockoff method. Moreover, the trend of the $model$ -X knockoff curve shows that the discrepancy in relative CPU time is likely to grow even further for larger values of p . Thus, the T -Knock filter can be easily scaled to large-scale high-dimensional settings while the $model$ -X knockoff method is practically infeasible in such settings. Note that both axes are scaled logarithmically. Setup: $n = 300$, $p_1 = 10$, $L = p$, $K = 20$, $SNR = 1$, $MC = 955$.

5. Simulated Genome-Wide Association Study

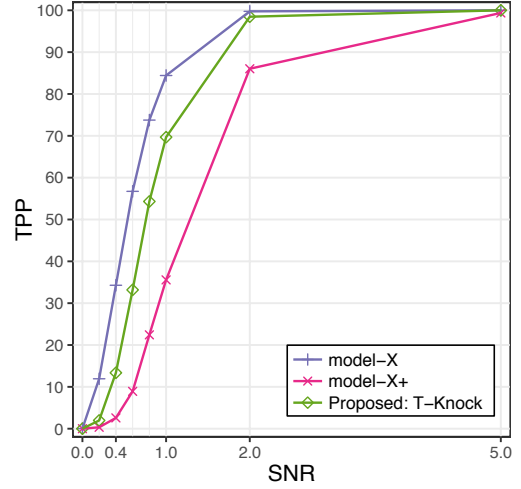
The T -Knock filter and the benchmark methods that have been presented in Section 4.1 are used to conduct a high-dimensional, but relatively small, simulated case-control genome-wide association study (GWAS). The goal is to detect the so-called single nucleotide polymorphisms (SNPs) that are associated with a disease (i.e., active variables), while keeping the number of selected SNPs that are not associated with the same disease (i.e., null variables) low. The data generation and preprocessing steps are described first, followed by a discussion of the results.

5.1 Setup

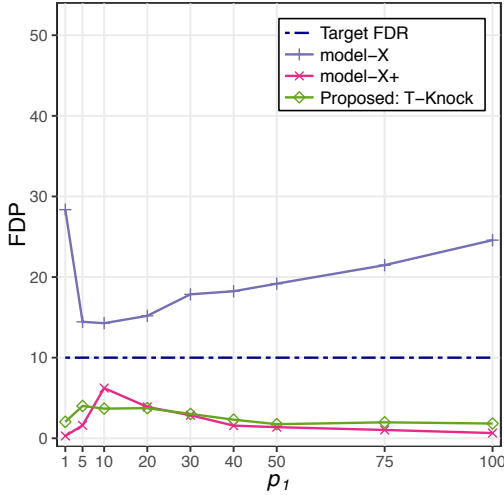
The genotypes of 700 cases and 300 controls are simulated based on haplotypes from phase 3 of the International HapMap project (Consortium, 2010) using the HAPGEN2 software (Su et al., 2011). We simulated 10 randomly selected disease loci on the first 20,000 SNPs of chromosome 15 (contains 42,351 in total) with randomly selected risk alleles (either 0 or 1 with $\mathbb{P}("0") = \mathbb{P}("1") = 0.5$) and with the heterozygote risks and the homozygote risks being sampled from the uniform distribution on the intervals $[1.5, 2]$ and $[2.5, 3]$, respectively. Since we are conducting a case-control study, the control and case phenotypes are 0 and 1, respectively. Note that the SNPs and the phenotypes represent the candidate variables and the responses, respectively, while the disease loci represent the indices of the active variables. Thus, we have $p_1 = 10$ active variables and $p_0 = 19,990$ null variables. The number of observations is $n = 1000$ (700 cases and 300 controls).



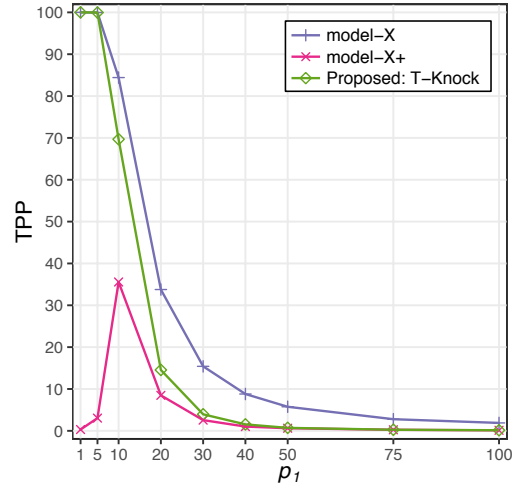
(a) The *T-Knock* filter and the *model-X knockoff+* method control the FDR at a target level of 10% for the whole range of SNR values while the *model-X knockoff* method fails to control the FDR and performs poorly at low SNR values. Setup: $n = 300$, $p = 1000$, $p_1 = 10$, $T_{\max} = \lceil n/2 \rceil$, $L_{\max} = 10p$, $K = 20$, $MC = 955$.



(b) As expected, the TPR (i.e., power) increases with respect to the SNR. It is remarkable that even though the FDR of the *T-Knock* filter lies below that of the *model-X knockoff+* method for SNR values larger than 0.6, its power exceeds that of its strongest FDR controlling competitor. The high power of the *model-X knockoff* method cannot be interpreted as an advantage, because the method does not control the FDR. Setup: Same as in Figure (a).



(c) As in Figure (a), only the *T-Knock* filter and the *model-X knockoff+* method control the FDR at a target level of 10%, while the curve of the *model-X knockoff* method never falls below the target level. Setup: $n = 300$, $p = 1000$, $T_{\max} = \lceil n/2 \rceil$, $L_{\max} = 10p$, $K = 20$, $\text{SNR} = 1$, $MC = 955$.



(d) Among the FDR controlling methods, the *T-Knock* filter has by far the highest power for sparse settings. The power of the *model-X knockoff* method exceeds that of the FDR controlling methods, but this cannot be interpreted as an advantage of the method since it exceeds the target FDR level. Note that for an increasing number of active variables the power drops for all methods since apparently the number of data points $n = 300$ does not suffice in the simulated settings with a low sparsity level, i.e., settings with many active variables. Setup: Same as in Figure (c).

Figure 8: The *model-X knockoff* method fails to control the FDR. Among the FDR controlling methods, the *T-Knock* filter outperforms the *model-X knockoff+* method in terms of power.

We simulate 100 data sets with the above described parameters. According to the authors, HAPGEN2 uses the time of the current day in seconds to set the seed of the random number generator, and, therefore multiple simulations should not be started very close in time to avoid identical results. Therefore we have generated the data sets sequentially and since generating a single dataset took roughly six minutes, a sufficient time period between the start of consecutive simulations was allowed.¹⁸

The preprocessing is carried out as suggested in (Sesia et al., 2019) and on the accompanying website.¹⁹ That is, SNPs with a minor allele frequency or call rate lower than 1% and 95%, respectively, are removed. Additionally, SNPs that violate the Hardy-Weinberg disequilibrium with a cutoff of 10^{-6} are removed. Since proximate SNPs are highly correlated, the remaining SNPs are clustered using a hierarchical clustering procedure that ensures that there exist no absolute sample correlations above 0.75 between any two SNPs belonging to different clusters. The resulting average number of clusters is 8211 while the minimum number 8120 is and the maximum number is 8326. Each cluster is represented by the strongest cluster representative which is selected by computing the marginal p -values using the Cochran-Armitage test based on 20% of the data and picking the SNP with the smallest p -value. The marginal p -values that will be plugged into the BH method and the BY method are also computed using the Cochran-Armitage test but with the full data set.

5.2 Results

The following simulation results allow to compare the performances of the proposed T -Knock filter in combination with the proposed extended calibration algorithm in Algorithm 2 with the benchmark methods. The detailed results and a discussion thereof are given in Figure 9 and Table 2.

6. Conclusion

The T -Knock filter, a fast variable selection method for high-dimensional settings that provably controls the FDR at the target level, was proposed. It fuses the results of multiple early terminated random experiments that are conducted on the computer by applying a forward selection method to the original data and artificially generated knockoff variables. One major motivation for developing the T -Knock filter is to detect as many as possible truly associated SNPs with a phenotype of interest in large scale genome-wide association studies (GWAS) in a reasonable amount of computation time. The T -Knock filter has not only shown that it is capable of performing variable selection with higher power than the only benchmark method that provably controls the FDR, namely the *model-X knockoff+* method, but also that its sequential computation time is multiple orders of magnitude lower than that of the strongest benchmark methods. Since the T -Knock random experiments can be computed in parallel, multicore computers and high performance clusters allow for additional substantial savings in computation time. These properties make the T -Knock filter a suitable method for reproducibility studies of large-scale GWAS.

As a next step, we will conduct multiple reproducibility studies applying the T -Knock filter on large-scale genotype and phenotype data from the UK Biobank (Sudlow et al., 2015) in order to reproduce some of the reported results in the GWAS catalog (Buniello et al., 2019). Our aim is to confirm past discoveries, discover new genetic associations, and flag potentially false reported genetic associations. We plan to publish our results as a curated catalog of reproducible genetic associations

18. The data sets were generated on a compute node of the Lichtenberg high performance cluster of the Technische Universität Darmstadt that consists of two “Intel[®] Xeon[®] Platinum 9242 Processors” with 96 cores and 384 GB RAM (DDR4-2933) in total.

19. URL: https://web.stanford.edu/group/candes/knockoffs/tutorials/gwas_tutorial.html (last access: September 23, 2021).

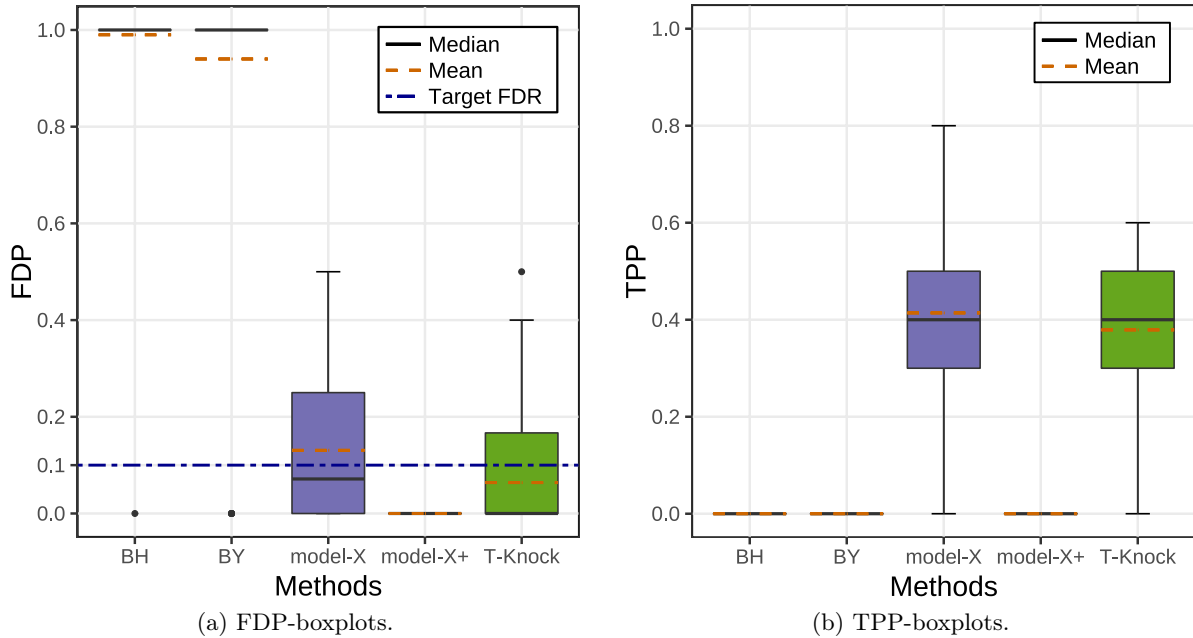


Figure 9: The proposed *T-Knock* filter is the only method that has an average FDR below the target FDR level and that has a non-zero power. Note that the FDR can be different across the realizations and even for FDR controlling methods it is not necessarily below the target level for every realization. We use boxplots to visualize the distribution of the results and give the reader a sense of how the FDR and TPP (i.e., power) vary around the mean.

and hope that this endeavor helps scientists to focus their efforts in revealing the causal mechanisms behind the genetic associations on the most promising and reproducible genetic associations.

Acknowledgments

The work of the first author has been funded by the Deutsche Forschungsgemeinschaft (DFG, German Research Foundation) under grant number 425884435.

The work of the second author has been funded by the LOEWE initiative (Hesse, Germany) within the emergenCITY center and is supported by the ‘Athene Young Investigator Programme’ of Technische Universität Darmstadt, Darmstadt, Germany.

The work of the third author has been funded by the Hong Kong GRF 16207820 research grant.

Extensive calculations on the Lichtenberg high-performance computer of the Technische Universität Darmstadt were conducted for this research. The authors would like to thank the Hessian Competence Center for High Performance Computing – funded by the Hessian Ministry of Higher Education, Research and the Arts – for helpful advice.

Appendices

The following supplementary material to the main paper is organized as follows: Appendix A provides numerical verifications of Assumptions 1, 2, and 3 while Appendix B gives detailed proofs

Methods	FDR control?	Average FDP (in %)	Average TPP (in %)	Sequential computation time (hh:mm:ss)	Relative Sequential computation time
Proposed: <i>T-Knock</i>	✓	6.39	37.90	00:03:02	1
<i>model-X+</i>	✓	0.00	0.00	12:32:00	247.03
<i>model-X</i>	✗	13.07	41.40	12:32:00	247.03
<i>BY</i>	✗	94.00	0.00	00:00:00	0.00
<i>BH</i>	✗	99.00	0.00	00:00:00	0.00

Table 2: The proposed *T-Knock* filter is the only method whose average FDP lies below the target FDR level of 10% while achieving a non-zero power. The only competitor that provably possesses the FDR control property, namely the *model-X* knockoff+ method, has an average FDP of 0% but also an average TPP of 0%, i.e., it has no power. The *model-X* knockoff method has a slightly higher power than the proposed *T-Knock* filter but it exceeds the target FDR level. In addition to outperforming its competitors, the sequential computation time of the proposed *T-Knock* filter in combination with the extended calibration algorithm in Algorithm 2 is roughly 3 minutes as compared to more than 12.5 hours for the *model-X* methods. That is, the *T-Knock* filter is 247 times faster than its strongest competitors. Note that this is only a comparison of the sequential computation times. Since the random experiments of the proposed *T-Knock* filter are independent and, therefore, can be run in parallel on a multicore computer or a high performance cluster, an additional substantial speedup can be achieved. As expected, the procedure of plugging the marginal p -values into the *BH* method or the *BY* method fails to control the FDR and to achieve a reasonable power in this high-dimensional setting. Note that computing marginal p -values for the *BH* method and the *BY* method is computationally cheap but the obtained p -values turn out to be ineffective when plugged into the *BH* method or the *BY* method.

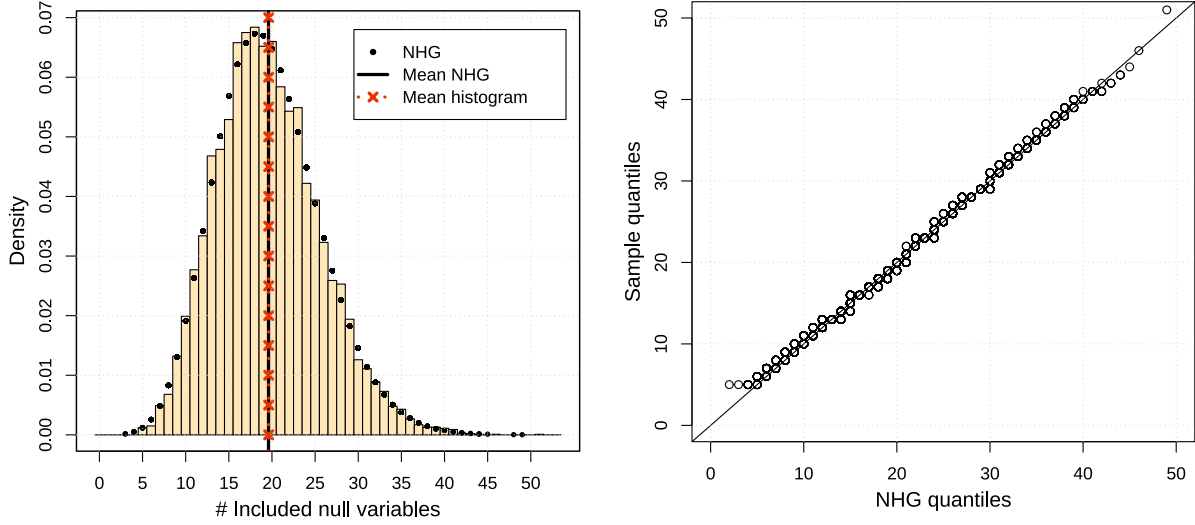
of Theorems 1, 2, and 3. In Appendix C, additional simulation results for a low-dimensional setting are presented and discussed.

Appendix A. Numerical Verification of Assumptions

The data for the numerical verification of all assumptions is generated as described in Section 4.2. The specific values of the generic simulation setting in Section 4.2 and the parameters of the proposed *T-Knock* filter and the proposed extended calibration algorithm in Algorithm 2, i.e., the values of n , p , p_1 , v , T , L , K , and SNR are specified in the figure captions. All results are averaged over 500 Monte Carlo realizations.

A.1 Verification of Assumption 1

Figure 10 (a) shows the histogram of the number of included null variables for $T = 20$ and for 500 Monte Carlo replications consisting of $K = 20$ candidate sets each while Figure 10 (b) shows the corresponding Q-Q plot. The histogram closely approximates the probability mass function (PMF) of the negative hypergeometric distribution with the parameters specified in Corollary 1. Moreover, the points in the Q-Q plot closely approximate the ideal line. Thus, Figure 10 provides a numerical verification of Corollary 1 and, therewith, an implicit verification of Assumption 1 in the considered setting.



(a) Histogram and theoretical distribution for $t = T = 20$. Note that the histogram is based on $K = 20$ random experiments for each of the 500 Monte Carlo realizations.

(b) Q-Q plot corresponding to Figure (a).

Figure 10: Verification of Corollary 1 and Assumption 1: The histogram of the number of included null variables in Figure (a) approximates the theoretical probability mass function (PMF). As mentioned in Remark 3, the expected value of a random variable following the negative hypergeometric distribution with the parameters specified in the last sentence of this caption is given by $T \cdot p_0 / (L + 1) = 20 \cdot 290 / (300 + 1) \approx 19.27$, which fits the mean of the histogram. The Q-Q plot in Figure (b) confirms that the number of included null variables follows the negative hypergeometric distribution. Setup: $n = 150$, $p = 300$, $p_1 = 5$, $T = 20$, $L = p$, $K = 20$, $\text{SNR} = 1$.

A.2 Verification of Assumption 2

Figure 11 shows the empirical cumulative distribution function (CDF) of $V_{T,L}(v)$ for $T = 20$ and different values of the voting level v and the CDF of the negative hypergeometric distribution. The empirical CDFs are based on 500 Monte Carlo replications. Already for a small number of random experiments, i.e., $K = 20$, the CDF of the negative hypergeometric distribution with its parameters being as specified in Assumption 2 lies below the empirical CDFs of $V_{T,L}(v)$ for all $v \geq 0.5$ at almost all values of $V_{T,L}(v)$. For values of $V_{T,L}(v)$ between 6 and 12, we observe that the CDF of the negative hypergeometric distribution lies slightly above the empirical CDF for $v = 0.5$. All in all, we conclude that a random variable following the negative hypergeometric distribution stochastically dominates $V_{T,L}(v)$ at almost all values and for all $v \geq 0.5$, which numerically verifies Assumption 2 in the considered setting.

A.3 Verification of Assumption 3

The expression for $\widehat{V}'_{T,L}(v)$ can be rewritten as follows:

$$\widehat{V}'_{T,L}(v) = \sum_{t=1}^T \frac{p - \sum_{q=1}^p \Phi_{t,L}(q)}{L - (t-1)} \cdot \frac{\sum_{j \in \widehat{\mathcal{A}}(v)} \Delta \Phi_{t,L}(j)}{\sum_{q \in \widehat{\mathcal{A}}(0.5)} \Delta \Phi_{t,L}(q)}$$

$$\begin{aligned}
&= \sum_{t=1}^T \frac{p_0 - \sum_{q \in \mathcal{Z}} \Phi_{t,L}(q) + \overbrace{p_1 - \sum_{q \in \mathcal{A}} \Phi_{t,L}(q)}^{\phantom{p_1 - \sum_{q \in \mathcal{A}} \Phi_{t,L}(q)}}}{L - (t - 1)} \\
&\quad \cdot \frac{\sum_{j \in \hat{\mathcal{A}}^0(v)} \Delta \Phi_{t,L}(j) + \overbrace{\sum_{j \in \hat{\mathcal{A}}^1(v)} \Delta \Phi_{t,L}(j)}^{\phantom{\sum_{j \in \hat{\mathcal{A}}^1(v)} \Delta \Phi_{t,L}(j)}}}{\sum_{q \in \hat{\mathcal{A}}^0(0.5)} \Delta \Phi_{t,L}(q) + \overbrace{\sum_{q \in \hat{\mathcal{A}}^1(0.5)} \Delta \Phi_{t,L}(q)}^{\phantom{\sum_{q \in \hat{\mathcal{A}}^1(0.5)} \Delta \Phi_{t,L}(q)}}} \\
&\approx \sum_{t=1}^T \frac{p_0 - \sum_{q \in \mathcal{Z}} \Phi_{t,L}(q)}{L - (t - 1)} \cdot \frac{\sum_{j \in \hat{\mathcal{A}}^0(v)} \Delta \Phi_{t,L}(j)}{\sum_{q \in \hat{\mathcal{A}}^0(0.5)} \Delta \Phi_{t,L}(q)}
\end{aligned}$$

The marked terms consider only the relative occurrences of the active variables. Recall that,

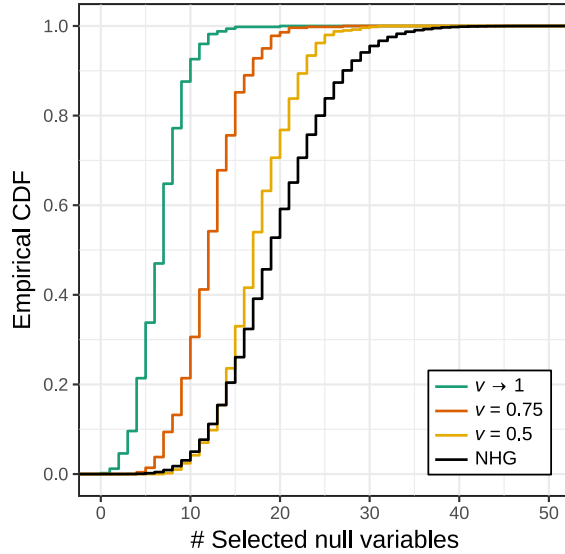
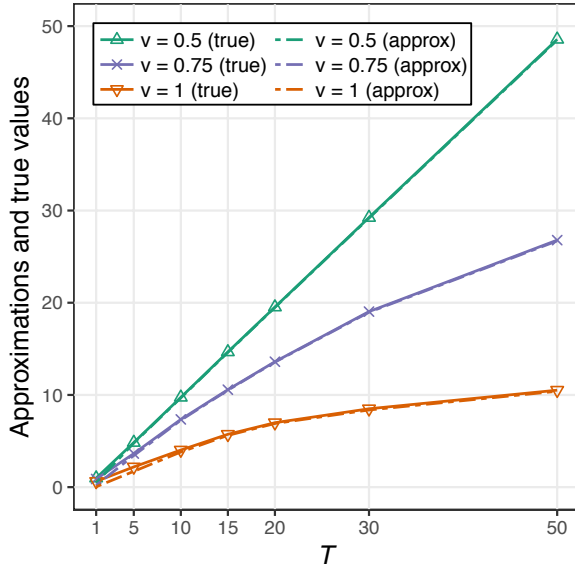


Figure 11: Verification of Assumption 2: For $v \geq 0.5$, a random variable following the negative hypergeometric distribution stochastically dominates the random variable $V_{T,L}(v)$, (i.e., the number of selected null variables) at almost all values of $V_{T,L}(v)$. Setup: $n = 150$, $p = 300$, $p_1 = 5$, $T = 20$, $L = p$, $K = 20$, $\text{SNR} = 1$.

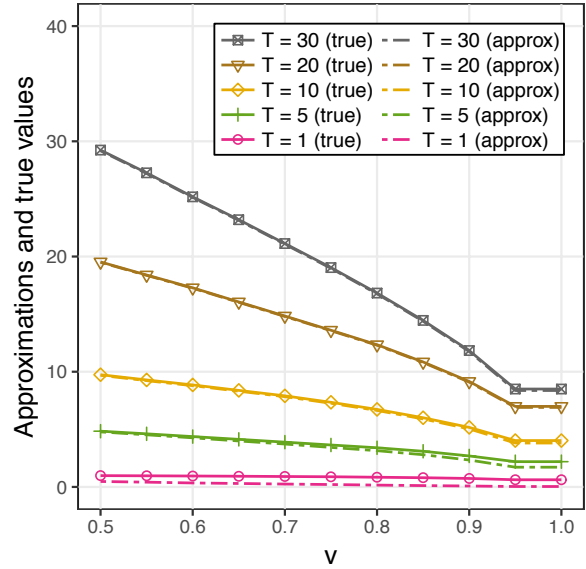
assuming that the variable selection method is better than random guessing, almost all active variables are selected early, i.e., terminating the T -Knock filter after a small number of T knockoffs have been included, allows to select almost all active variables (see Figure 4 (a)). Thus, the relative occurrences of the active variables are approximately one for a sufficient number of included knockoffs. In consequence, and since $\Delta \Phi_{t,L} = \Phi_{t,L} - \Phi_{t-1,L}$, $t \in \{1, \dots, T\}$, the $\Delta \Phi_{t,L}$'s of the active variables are approximately zero for a sufficiently large t and T . This motivates the assumption that the marked terms can be neglected. A numerical verification of this assumption is given in Figure 12, where we see that approximations and true values are almost identical for different choices of v and T .

Appendix B. Proofs

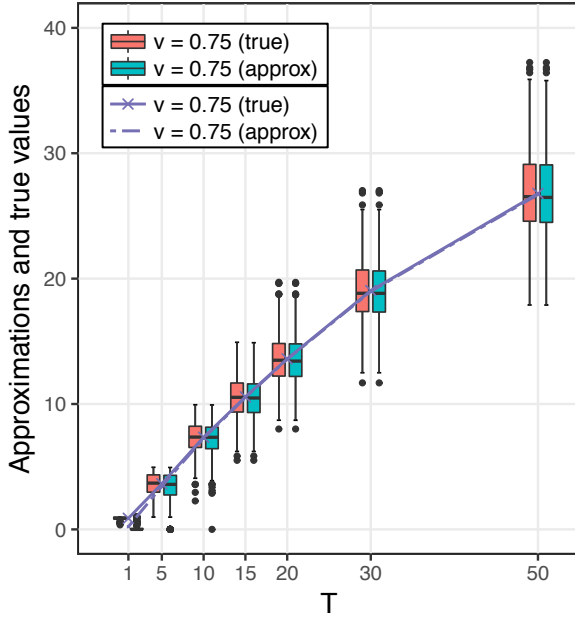
In this appendix, we introduce and prove some preliminary technical results. Then, the detailed proofs of Theorem 1 (FDR control), Theorem 2 (Knockoff generation), and Theorem 3 (Optimality of Algorithm 1) are presented.



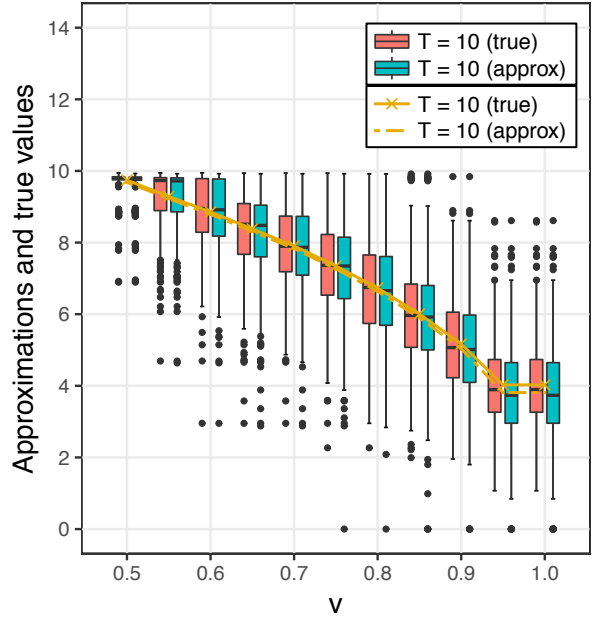
(a) Approximations and true values for different choices of v averaged over 500 Monte Carlo realizations.



(b) Approximations and true values for different choices of T averaged over 500 Monte Carlo realizations.



(c) Boxplots of approximations and true values corresponding to the lines for $v = 0.75$ in Figure (a).



(d) Boxplots of approximations and true values corresponding to the lines for $T = 10$ in Figure (b).

Figure 12: Verification of Assumption 3: In Figures (a) and (b), we see that that the approximations and the true values are almost identical for different values of v and T . The corresponding boxplots in Figures (c) and (d) show that also the distributions of approximations and true values are very similar.

B.1 Preliminaries: Technical Lemmas and Corollaries

As a consequence of Assumptions 1 and 2, the number of selected null variables (i.e., $V_{T,L}(v)$) conditioned on the number of null variables exceeding the minimum voting level of 50% (i.e., $V_{T,L}(0.5)$) is binomially distributed with $\mathbb{P}(\Phi_{T,L}(j_0) > v)$ being the selection probability of variable $j_0 \in \widehat{\mathcal{A}}^0(0.5)$. Thus, we obtain the following hierarchical model:

Corollary 2. *The number of selected null variables $V_{T,L}(v)$ follows the hierarchical model*

$$V_{T,L}(v) \mid V_{T,L}(0.5) \sim \text{Binomial}\left(V_{T,L}(0.5), \mathbb{P}(\Phi_{T,L}(j_0) > v)\right),$$

$$V_{T,L}(0.5) \stackrel{d}{\leq} \text{NHG}(p_0 + L, p_0, T),$$

where $\mathbb{P}(\Phi_{T,L}(j_0) > v) > 0$ for all $j_0 \in \widehat{\mathcal{A}}^0(0.5)$ and for any $v \in [0.5, 1)$.

Lemma 1. *Let v be any real number in $[0.5, 1)$ and $K \rightarrow \infty$. Then, for any $j_0 \in \widehat{\mathcal{A}}^0(0.5)$, the following equation is satisfied:*

$$\mathbb{E}[V_{T,L}(v)] = \mathbb{P}(\Phi_{T,L}(j_0) > v) \cdot \mathbb{E}[V_{T,L}(0.5)].$$

Proof. Using the tower property of the expectation, we can rewrite the expectation of $V_{T,L}(v)$ as follows:

$$\begin{aligned} \mathbb{E}[V_{T,L}(v)] &= \mathbb{E}\left[\mathbb{E}[V_{T,L}(v) \mid V_{T,L}(0.5)]\right] \\ &= \mathbb{E}[V_{T,L}(0.5) \cdot \mathbb{P}(\Phi_{T,L}(j_0) > v)] \\ &= \mathbb{P}(\Phi_{T,L}(j_0) > v) \cdot \mathbb{E}[V_{T,L}(0.5)]. \end{aligned}$$

The second equation follows from

$$V_{T,L}(v) \mid V_{T,L}(0.5) \sim \text{Binomial}\left(V_{T,L}(0.5), \mathbb{P}(\Phi_{T,L}(j_0) > v)\right)$$

in Corollary (2) and the third equation holds because $\Phi_{T,L}(j_0)$, $j_0 \in \widehat{\mathcal{A}}^0(0.5)$, are i.i.d. random variables and, therefore, the selection probability $\mathbb{P}(\Phi_{T,L}(j_0) > v)$ for any fixed v is the same constant for all j_0 . \square

Lemma 2. *Let v be any real number in $[0.5, 1)$ and $K \rightarrow \infty$. Define*

$$\widehat{V}'_{T,L}(v) := \widehat{V}_{T,L}(v) - \sum_{j \in \widehat{\mathcal{A}}(v)} (1 - \Phi_{T,L}(j)).$$

Suppose that Assumptions 1 and 3 hold. Then, for any $j_0 \in \widehat{\mathcal{A}}^0(0.5)$, the following equation is satisfied:

$$\mathbb{E}[\widehat{V}'_{T,L}(v)] = \mathbb{P}(\Phi_{T,L}(j_0) > v) \cdot \widehat{V}'_{T,L}(0.5).$$

Proof. Taking the expectation of $\widehat{V}_{T,L}(v)$ yields

$$\begin{aligned} \mathbb{E}[\widehat{V}'_{T,L}(v)] &= \mathbb{E}\left[\sum_{t=1}^T \frac{p - \sum_{q=1}^p \Phi_{t,L}(q)}{L - (t-1)} \cdot \frac{\sum_{j \in \widehat{\mathcal{A}}(v)} \Delta \Phi_{t,L}(j)}{\sum_{q \in \widehat{\mathcal{A}}(0.5)} \Delta \Phi_{t,L}(q)}\right] \\ &= \sum_{t=1}^T \frac{p_0 - \sum_{q \in \mathcal{Z}} \Phi_{t,L}(q)}{L - (t-1)} \cdot \mathbb{E}\left[\frac{\sum_{j \in \widehat{\mathcal{A}}^0(v)} \Delta \Phi_{t,L}(j)}{\sum_{q \in \widehat{\mathcal{A}}^0(0.5)} \Delta \Phi_{t,L}(q)}\right], \end{aligned} \quad (12)$$

where the first and the second equation follow from Definitions 5 and 6. Note that $\sum_{q \in \mathcal{Z}} \Phi_{t,L}(q) = \frac{1}{K} \sum_{k=1}^K \sum_{q \in \mathcal{Z}} \mathbb{1}_k(q, t, L)$, i.e., the average number of included null variables when stopping after t knockoffs have been included. Since $K \rightarrow \infty$, the law of large numbers allows us to replace the average by its expectation. That is, $\sum_{q \in \mathcal{Z}} \Phi_{t,L}(q) = \mathbb{E}[\sum_{q \in \mathcal{Z}} \mathbb{1}_k(q, t, L)]$, where the expectation is taken with respect to the distribution of the knockoffs. Moreover, since $\sum_{q \in \mathcal{Z}} \mathbb{1}_k(q, t, L)$ is independent of the noise in the linear model, $\mathbb{E}[\sum_{q \in \mathcal{Z}} \mathbb{1}_k(q, t, L)]$ is also independent of the noise in the linear model. Therefore, $\sum_{q \in \mathcal{Z}} \Phi_{t,L}(q)$ is deterministic and can be written outside the expectation.

Using the tower property, we can rewrite the expectation in (12) as follows:

$$\begin{aligned} \mathbb{E}\left[\frac{\sum_{j \in \widehat{\mathcal{A}}^0(v)} \Delta \Phi_{t,L}(j)}{\sum_{q \in \widehat{\mathcal{A}}^0(0.5)} \Delta \Phi_{t,L}(q)}\right] &= \mathbb{E}\left[\mathbb{E}\left[\frac{\sum_{j \in \widehat{\mathcal{A}}^0(v)} \Delta \Phi_{t,L}(j)}{\sum_{q \in \widehat{\mathcal{A}}^0(0.5)} \Delta \Phi_{t,L}(q)} \mid |\widehat{\mathcal{A}}^0(v)|, |\widehat{\mathcal{A}}^0(0)|\right]\right] \\ &= \mathbb{E}\left[\frac{|\widehat{\mathcal{A}}^0(v)|}{|\widehat{\mathcal{A}}^0(0.5)|}\right] \end{aligned} \quad (13)$$

The last equation follows from $\Delta \Phi_{t,L}(j_0)$, $j_0 \in \widehat{\mathcal{A}}^0(0.5)$, being i.i.d. random variables and the well known fact that $\mathbb{E}[Q_M / Q_N] = M / N$, where $Q_M = \sum_{m=1}^M Z_m$ with Z_1, \dots, Z_M being non-zero i.i.d. random variables and $M \leq N$.

Noting that $|\widehat{\mathcal{A}}^0(v)| = V_{T,L}(v)$ and applying the tower property again, we can rewrite the expectation in (13) as follows:

$$\begin{aligned} \mathbb{E}\left[\frac{|\widehat{\mathcal{A}}^0(v)|}{|\widehat{\mathcal{A}}^0(0.5)|}\right] &= \mathbb{E}\left[\frac{V_{T,L}(v)}{V_{T,L}(0.5)}\right] \\ &= \mathbb{E}\left[\mathbb{E}\left[\frac{V_{T,L}(v)}{V_{T,L}(0.5)} \mid V_{T,L}(0.5)\right]\right] \\ &= \mathbb{E}\left[\frac{1}{V_{T,L}(0.5)} \cdot \mathbb{E}[V_{T,L}(v) \mid V_{T,L}(0.5)]\right] \\ &= \mathbb{E}\left[\frac{1}{V_{T,L}(0.5)} \cdot V_{T,L}(0.5) \cdot \mathbb{P}(\Phi_{T,L}(j_0) > v)\right] \\ &= \mathbb{P}(\Phi_{T,L}(j_0) > v). \end{aligned}$$

The last three equations follow from the same arguments as in the proof of Lemma 1. Thus,

$$\begin{aligned}\mathbb{E}[\widehat{V}'_{T,L}(v)] &= \mathbb{P}(\Phi_{T,L}(j_0) > v) \cdot \sum_{t=1}^T \frac{p - \sum_{q=1}^p \Phi_{t,L}(q)}{L - (t-1)} \\ &= \mathbb{P}(\Phi_{T,L}(j_0) > v) \cdot \widehat{V}'_{T,L}(0.5).\end{aligned}$$

□

Lemma 3. *Let $K \rightarrow \infty$. Then,*

$$\mathbb{E}\left[\sum_{q \in \mathcal{Z}} \Phi_{t,L}(q)\right] = \frac{t}{L+1} \cdot p_0.$$

Proof. Using Definition 1, we obtain

$$\sum_{j \in \mathcal{Z}} \Phi_{t,L}(q) = \frac{1}{K} \sum_{k=1}^K \sum_{q \in \mathcal{Z}} \mathbb{1}_k(j, t, L).$$

Then, taking the expectation and noting that

$$\sum_{j \in \mathcal{Z}} \mathbb{1}_k(j, t, L) \sim \text{NHG}(p_0 + L, p_0, t), \quad k = 1, \dots, K,$$

i.e., the number of included null variables in the K random experiments are i.i.d. random variables following the negative hypergeometric distribution as stated in Corollary 1, yields

$$\begin{aligned}\mathbb{E}\left[\sum_{q \in \mathcal{Z}} \Phi_{t,L}(q)\right] &= \frac{1}{K} \sum_{k=1}^K \mathbb{E}\left[\sum_{q \in \mathcal{Z}} \mathbb{1}_k(q, t, L)\right] \\ &= \frac{1}{K} \cdot K \cdot \frac{t}{L+1} \cdot p_0 \\ &= \frac{t}{L+1} \cdot p_0.\end{aligned}$$

□

Lemma 4. *Let v be any real number in $[0.5, 1)$. Define*

$$\epsilon_{T,L}^*(v) := \inf\{\epsilon \in (0, v) : R_{T,L}(v - \epsilon) - R_{T,L}(v) = 1\} \quad (14)$$

with the convention that $\epsilon_{T,L}^(v) = 0$ if the infimum does not exist. Suppose that $V_{T,L}(v - \epsilon_{T,L}^*(v)) = V_{T,L}(v) + 1$, $\mathbb{E}[V_{T,L}(v)] > 0$, and $\mathbb{E}[\widehat{V}'_{T,L}(v)] > 0$. Then, for all $j_0 \in \widehat{\mathcal{A}}^0(0.5)$ it holds that*

$$(i) \quad \mathbb{E}[V_{T,L}(v - \epsilon_{T,L}^*(v)) \mid V_{T,L}(v)] = V_{T,L}(v) \cdot \frac{\mathbb{P}(\Phi_{T,L}(j_0) > v - \epsilon_{T,L}^*(v))}{\mathbb{P}(\Phi_{T,L}(j_0) > v)}$$

and

$$(ii) \quad \mathbb{E}[\widehat{V}'_{T,L}(v - \epsilon_{T,L}^*(v)) \mid \widehat{V}'_{T,L}(v)] = \widehat{V}'_{T,L}(v) \cdot \frac{\mathbb{P}(\Phi_{T,L}(j_0) > v - \epsilon_{T,L}^*(v))}{\mathbb{P}(\Phi_{T,L}(j_0) > v)}.$$

Proof. (i) Let $\delta \geq 1$ be a constant that satisfies the equation $V_{T,L}(v - \epsilon_{T,L}^*(v)) = \delta \cdot V_{T,L}(v)$. Then,

$$\mathbb{E}[V_{T,L}(v - \epsilon_{T,L}^*(v)) \mid V_{T,L}(v)] = \mathbb{E}[\delta \cdot V_{T,L}(v) \mid V_{T,L}(v)] = \delta \cdot V_{T,L}(v).$$

We rewrite $\delta \cdot V_{T,L}(v)$ as follows:

$$\begin{aligned} \delta \cdot V_{T,L}(v) &= V_{T,L} \cdot \frac{\delta \cdot \mathbb{E}[V_{T,L}(v)]}{\mathbb{E}[V_{T,L}(v)]} \\ &= V_{T,L} \cdot \frac{\delta \cdot \mathbb{E}[V_{T,L}(v - \epsilon_{T,L}^*(v))]}{\mathbb{E}[V_{T,L}(v)]} \\ &= V_{T,L} \cdot \frac{\mathbb{P}(\Phi_{T,L}(j_0) > v - \epsilon_{T,L}^*(v))}{\mathbb{P}(\Phi_{T,L}(j_0) > v)}. \end{aligned}$$

The last line follows from Lemma 1. Comparing $\delta \cdot V_{T,L}(v)$ and the last line, we see that $\delta = \mathbb{P}(\Phi_{T,L}(j_0) > v - \epsilon_{T,L}^*(v)) / \mathbb{P}(\Phi_{T,L}(j_0) > v)$ and the first part of the lemma follows.

(ii) The proof is analogous to the proof of (i). The only difference is that Lemma 2 instead of Lemma 1 needs to be used for rewriting the expression $\delta \cdot \widehat{V}'_{T,L}(v)$. \square

B.2 Lemma 5 (Martingale)

Lemma 5. Define $\mathcal{V} := \{\Phi_{T,L}(j) : \Phi_{T,L}(j) > 0.5, j = 1, \dots, p\}$ and

$$H_{T,L}(v) := \frac{V_{T,L}(v)}{\widehat{V}'_{T,L}(v)}.$$

Let $\mathcal{F}_v := \sigma(\{V_{T,L}(u)\}_{u \geq v}, \{\widehat{V}'_{T,L}(u)\}_{u \geq v})$ be a backward-filtration with respect to v . Suppose that Assumption 3 holds. Then, for all tuples $(T, L) \in \{1, \dots, L\} \times \mathbb{N}_+$, $\{H_{T,L}(v)\}_{v \in \mathcal{V}}$ is a backward-running super-martingale with respect to \mathcal{F}_v . That is,

$$\mathbb{E}[H_{T,L}(v - \epsilon_{T,L}^*(v)) \mid \mathcal{F}_v] \geq H_{T,L}(v).$$

Proof. If there exists a variable with index, say, j^* that is not selected at the voting level v but at the level $v - \epsilon_{T,L}^*(v)$ and it is a null variable, then we have

$$V_{T,L}(v - \epsilon_{T,L}^*(v)) = V_{T,L}(v) + 1.$$

However, if j^* is an active variable or if the infimum in (14) does not exist, that is, no additional variable is selected at the voting level $v - \epsilon_{T,L}^*(v)$ when compared to the level v , then we obtain

$$V_{T,L}(v - \epsilon_{T,L}^*(v)) = V_{T,L}(v).$$

Summarizing both results, we have

$$V_{T,L}(v - \epsilon_{T,L}^*(v)) = \begin{cases} V_{T,L}(v) + 1, & j^* \in \mathcal{Z} \\ V_{T,L}(v), & j^* \in \mathcal{A} \text{ or } \epsilon_{T,L}^*(v) = 0 \end{cases}.$$

Thus, using the definition of $H_{T,L}(v)$ within Lemma 1, we obtain

$$\begin{aligned}
\mathbb{E}[H_{T,L}(v - \epsilon_{T,L}^*(v)) \mid \mathcal{F}_v] &= \mathbb{E}\left[\frac{V_{T,L}(v - \epsilon_{T,L}^*(v))}{\widehat{V}'_{T,L}(v - \epsilon_{T,L}^*(v))} \mid V_{T,L}(v), \widehat{V}'_{T,L}(v)\right] \\
&= \begin{cases} \mathbb{E}\left[\frac{V_{T,L}(v) + 1}{\widehat{V}'_{T,L}(v - \epsilon_{T,L}^*(v))} \mid V_{T,L}(v), \widehat{V}'_{T,L}(v)\right], & j^* \in \mathcal{Z} \\ \mathbb{E}\left[\frac{V_{T,L}(v)}{\widehat{V}'_{T,L}(v)} \mid V_{T,L}(v), \widehat{V}'_{T,L}(v)\right], & j^* \in \mathcal{A} \\ & \text{or } \epsilon_{T,L}^*(v) = 0 \end{cases} \\
&= \begin{cases} (V_{T,L}(v) + 1) \cdot \mathbb{E}\left[\frac{1}{\widehat{V}'_{T,L}(v - \epsilon_{T,L}^*(v))} \mid V_{T,L}(v), \widehat{V}'_{T,L}(v)\right], & j^* \in \mathcal{Z} \\ \frac{V_{T,L}(v)}{\widehat{V}'_{T,L}(v)}, & j^* \in \mathcal{A} \\ & \text{or } \epsilon_{T,L}^*(v) = 0 \end{cases}. \quad (15)
\end{aligned}$$

Using Lemma 4, we can rewrite the first factor within the first case of Equation (15) as follows:

$$\begin{aligned}
V_{T,L}(v) + 1 &= \mathbb{E}[V_{T,L}(v - \epsilon_{T,L}^*(v)) \mid V_{T,L}(v)] \\
&= V_{T,L}(v) \cdot \frac{\mathbb{P}(\Phi_{T,L}(j_0) > v - \epsilon_{T,L}^*(v))}{\mathbb{P}(\Phi_{T,L}(j_0) > v)}. \quad (16)
\end{aligned}$$

Next, we rewrite the second factor within the first case of Equation (15) as follows:

$$\begin{aligned}
\mathbb{E}\left[\frac{1}{\widehat{V}'_{T,L}(v - \epsilon_{T,L}^*(v))} \mid V_{T,L}(v), \widehat{V}'_{T,L}(v)\right] &\geq \frac{1}{\mathbb{E}[\widehat{V}'_{T,L}(v - \epsilon_{T,L}^*(v)) \mid V_{T,L}(v), \widehat{V}'_{T,L}(v)]} \\
&= \frac{1}{\mathbb{E}[\widehat{V}'_{T,L}(v - \epsilon_{T,L}^*(v)) \mid \widehat{V}'_{T,L}(v)]} \\
&= \left(\widehat{V}'_{T,L}(v) \cdot \frac{\mathbb{P}(\Phi_{T,L}(j_0) > v - \epsilon_{T,L}^*(v))}{\mathbb{P}(\Phi_{T,L}(j_0) > v)}\right)^{-1} \quad (17)
\end{aligned}$$

The first line follows from Jensen's inequality. The second line holds because $\widehat{V}'_{T,L}(v - \epsilon_{T,L}^*(v))$ and $V_{T,L}(v)$ are conditionally independent given $\widehat{V}'_{T,L}(v)$ and the last line follows from Lemma 4. Plugging (16) and (17) into (15) yields

$$\mathbb{E}[H_{T,L}(v - \epsilon_{T,L}^*(v)) \mid \mathcal{F}_v] \geq H_{T,L}(v),$$

i.e., $\{H_{T,L}(v)\}_{v \in \mathcal{V}}$, with $\mathcal{V} = \{\Phi_{T,L}(j) : j = 1, \dots, p\}$, is a backward-running super-martingale with respect to the filtration \mathcal{F}_v . \square

B.3 Proof of Theorem 1 (FDR control)

Proof. With Lemma 5 and since the stopping time in (9) is adapted, i.e., it is \mathcal{F}_v -measurable, the optional stopping theorem can be applied to upper bound $\mathbb{E}[H_{T,L}(v)]$. This yields, as $K \rightarrow \infty$,

$$\begin{aligned} \mathbb{E}[H_{T,L}(v)] &\leq \mathbb{E}[H_{T,L}(0.5)] \\ &= \frac{1}{\widehat{V}'_{T,L}(0.5)} \cdot \mathbb{E}[V_{T,L}(0.5)] \\ &\leq \frac{1}{\widehat{V}'_{T,L}(0.5)} \cdot \frac{T}{L+1} \cdot p_0 \\ &= \frac{1}{\frac{T}{L+1} \cdot p_0} \cdot \frac{T}{L+1} \cdot p_0 \\ &= 1. \end{aligned}$$

The first line is a consequence of the optional stopping theorem and Lemma 5 and the second line follows from $\widehat{V}'_{T,L}(0.5)$ being deterministic as $K \rightarrow \infty$. The third line follows because $V_{T,L}(v)$ is stochastically dominated by a random variable following the negative hypergeometric distribution as stated in Assumption 2. The fourth line holds since

$$\begin{aligned} \widehat{V}'_{T,L}(v) &= \sum_{t=1}^T \frac{p_0 - \sum_{q \in \mathcal{Z}} \Phi_{t,L}(q)}{L - (t-1)} \\ &= \sum_{t=1}^T \frac{p_0 - \frac{t}{L+1} \cdot p_0}{L - (t-1)} \\ &= \frac{p_0}{L+1} \cdot \sum_{t=1}^T \frac{L-t+1}{L-t+1}, \\ &= \frac{T}{L+1} \cdot p_0, \end{aligned}$$

where the second equation follows from Lemma 3. Finally, it follows

$$\begin{aligned} \text{FDR}(v, T, L) &= \mathbb{E}[\text{FDP}(v, T, L)] \\ &\leq \alpha \cdot \mathbb{E}[H_{T,L}(v)] \\ &\leq \alpha, \end{aligned}$$

i.e., FDR control at the target level α . □

B.4 Proof of Theorem 2 (Knockoff generation)

Proof. Since

$$\mathbb{E}[D_{n,l,m,k}] = \frac{1}{\Gamma_{n,m,k}} \cdot \sum_{i=1}^n \gamma_{i,m,k} \cdot \mathbb{E}[\mathring{X}_{i,l,k}] = 0$$

and

$$\text{Var} [D_{n,l,m,k}] = \frac{1}{\Gamma_{n,m,k}^2} \cdot \sum_{i=1}^n \gamma_{i,m,k}^2 \cdot \text{Var} [\mathring{X}_{i,l,k}] = 1$$

the Lindeberg-Feller central limit theorem can be used to prove that $D_{n,l,m,k} \xrightarrow{d} D$, $D \sim \mathcal{N}(0, 1)$. In order to do this, we define

$$\mathring{Q}_{i,l,m,k} := \frac{\gamma_{i,m,k} \cdot \mathring{X}_{i,l,k}}{\Gamma_{n,m,k}},$$

and check whether it satisfies the Lindeberg condition, i.e., whether

$$\lim_{n \rightarrow \infty} \sum_{i=1}^n \mathbb{E} \left[\mathring{Q}_{i,l,m,k}^2 \cdot I(|\mathring{Q}_{i,l,m,k}| > \tau) \right] = 0$$

holds. Rewriting the Lindeberg condition using the definition of $\mathring{Q}_{i,l,m,k}$ yields

$$\lim_{n \rightarrow \infty} \sum_{i=1}^n \left(\frac{\gamma_{i,m,k}}{\Gamma_{n,m,k}} \right)^2 \cdot \mathbb{E} \left[\mathring{X}_{i,l,k}^2 \cdot I \left(|\mathring{X}_{i,l,k}| > \frac{\tau \cdot \Gamma_{n,m,k}}{|\gamma_{i,m,k}|} \right) \right] = 0,$$

where $I(\cdot)$ denotes the indicator function, i.e., $I(A > B)$ is equal to one if $A > B$ and equal to zero if $A \leq B$. Since

$$\lim_{n \rightarrow \infty} \max_{1 \leq i \leq n} \left(\frac{\gamma_{i,m,k}}{\Gamma_{n,m,k}} \right)^2 = 0$$

and

$$\lim_{n \rightarrow \infty} \min_{1 \leq i \leq n} \left(\frac{\Gamma_{n,m,k}}{|\gamma_{i,m,k}|} \right) \rightarrow \infty,$$

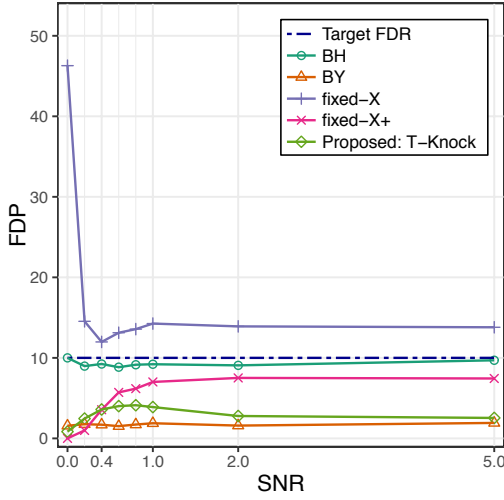
the Lindeberg condition is satisfied and the theorem follows. \square

B.5 Proof of Theorem 3 (Optimality of Algorithm 1)

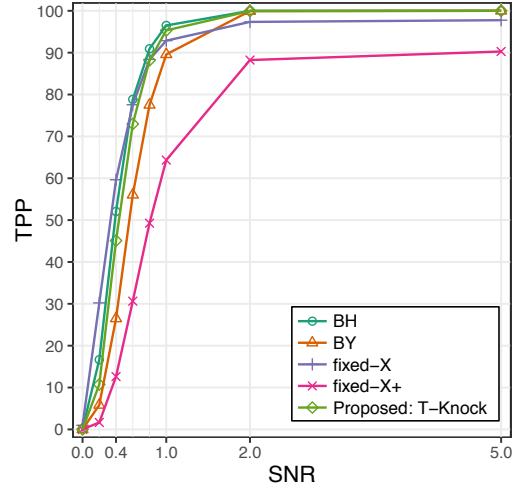
Proof. First, note that the objective functions in Step 4 of Algorithm 1 and in the optimization problem in (7) are equivalent, i.e., $|\widehat{\mathcal{A}}_L(v, T)| = R_{T,L}(v)$. Thus, in order to prove that (v^*, T^*) is an optimal solution of (7) it must be shown that the set of feasible tuples obtained by the algorithm contains the set $\{(v, T) : \widehat{\text{FDP}}(v, T, L) \leq \alpha\}$. This also proves that (v^*, T^*) is a feasible solution of (5) and (6) because the conditions of the optimization problems in (5), (6), and (7) are equivalent.

Since $\widehat{\text{FDP}}(v, T, L)$ is monotonically decreasing in v , for any $T \in \{1, \dots, L\}$, the minimum of $\widehat{\text{FDP}}(v, T, L)$ is attained at $v = 1 - \Delta v$. Moreover, $\widehat{\text{FDP}}(v, T, L)$ is monotonically increasing in T . Therefore, if $T_{\text{fin}} \in \{1, \dots, L\}$ satisfies the inequalities $\widehat{\text{FDP}}(v = 1 - \Delta v, T = T_{\text{fin}}, L) \leq \alpha$ and $\widehat{\text{FDP}}(v = 1, T = T_{\text{fin}} + 1, L) > \alpha$, then there exists no $v \in [0.5, 1)$ for $T = T_{\text{fin}}$ that satisfies $\widehat{\text{FDP}}(v, T, L) \leq \alpha$. Thus, the feasible set of (7) can be rewritten as follows:

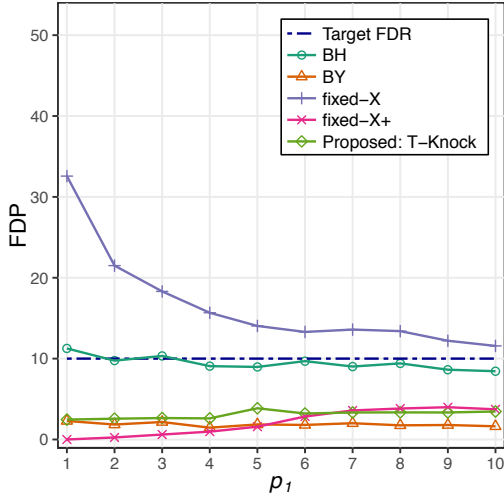
$$\begin{aligned} \{(v, T) : \widehat{\text{FDP}}(v, T, L) \leq \alpha\} = \\ \{(v, T) : v \in [0.5, 1), T \in \{1, \dots, T_{\text{fin}} - 1\}\} \\ \cup \{(v, T) : v \in \{\tilde{v} \in [0.5, 1) : \widehat{\text{FDP}}(\tilde{v}, T = T_{\text{fin}}, L) \leq \alpha\}, T = T_{\text{fin}}\}. \end{aligned} \quad (18)$$



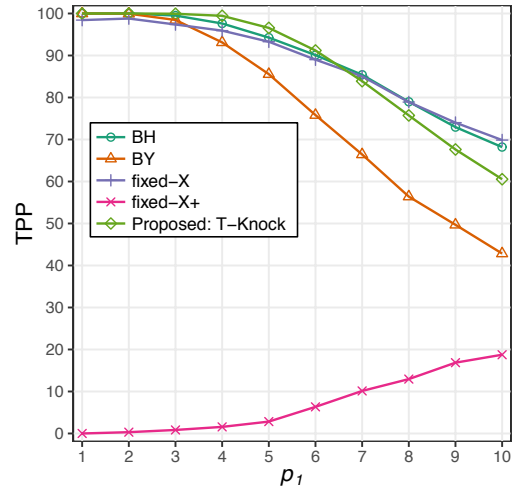
(a) All methods except for the *fixed-X knockoff* method control the FDR at a target level of 10% for the whole range of SNR values. The *fixed-X knockoff* method fails to control the FDR and performs poorly at low SNR values. Setup: $n = 300$, $p = 100$, $p_1 = 10$, $T_{\max} = \lceil n/2 \rceil$, $L_{\max} = 10p$, $K = 20$.



(b) As expected, the TPR (i.e., power) increases with respect to the SNR. It is remarkable that the TPP (i.e., power) of the proposed *T-Knock* filter is comparable to that of the *BH* method, although the FDR of the *T-Knock* filter is less than half of the achieved FDR of the *BH* method (see Figure (a)). The high power of the *fixed-X knockoff* method cannot be interpreted as an advantage, because the method does not control the FDR. Setup: Same as in Figure (a).



(c) The proposed *T-Knock* filter, the *fixed-X knockoff+* method, and the *BY* method control the FDR at a target level of 10%, while the *BH* method exceeds the target level for some low values of p_1 and the curve of the *fixed-X knockoff* method never falls below the target level. Setup: $n = 300$, $p = 100$, $T_{\max} = \lceil n/2 \rceil$, $L_{\max} = 10p$, $K = 20$, $\text{SNR} = 1$.



(d) Among the the methods that control the FDR for all considered values of p_1 , the proposed *T-Knock* filter has the highest power. It is remarkable that the TPP (i.e., power) of the proposed *T-Knock* filter is comparable to that of the *BH* method, although the FDR of the *T-Knock* filter is approximately only half of the achieved FDR of the *BH* method (see Figure (c)). Setup: Same as in Figure (c).

Figure 13: The *fixed-X knockoff* method fails to control the FDR. In terms of power, the proposed *T-Knock* filter outperforms the *fixed-X knockoff* method, the *fixed-X knockoff+* method, and the *BY* method and shows a comparable performance to the *BH* method.

The “while”-loop in Step 3 of Algorithm 1 is terminated when $T = T_{\text{fin}} + 1$. Thus, the feasible set of the optimization problem in Step 4 can be written as follows:

$$\{(v, T) : v \in [0.5, 1), T \in \{1, \dots, T_{\text{fin}}\}\}. \quad (19)$$

Since (18) is a subset of (19), the theorem follows. \square

Appendix C. Additional simulation results

For the sake of completeness, we present additional simulation results for the classical low-dimensional setting, i.e., $p \geq n$. The data is generated as described in Section 4.2. The specific values of the generic simulation setting in Section 4.2 and the parameters of the proposed T-Knock filter and the proposed extended calibration algorithm in Algorithm 2, i.e., the values of n , p , p_1 , T_{max} , L_{max} , K , and SNR are specified in the captions of Figure 13. All results are averaged over 955 Monte Carlo realizations. All in all, the proposed *T-Knock* filter controls the FDR at the target level of 10%, while, in terms of power, outperforming the *fixed-X* knockoff method, the *fixed-X knockoff+* method, and the *BY* method and showing a comparable performance to the *BH* method. A detailed discussion of the simulation results is given in the captions of Figure 13 and its subfigures.

References

- Rina Foygel Barber and Emmanuel J Candès. Controlling the false discovery rate via knockoffs. *The Annals of Statistics*, 43(5):2055–2085, 2015.
- Rina Foygel Barber and Emmanuel J Candès. A knockoff filter for high-dimensional selective inference. *The Annals of Statistics*, 47(5):2504–2537, 2019.
- Yoav Benjamini and Yosef Hochberg. Controlling the false discovery rate: a practical and powerful approach to multiple testing. *Journal of the Royal Statistical Society: Series B (Statistical Methodology)*, 57(1):289–300, 1995.
- Yoav Benjamini and Daniel Yekutieli. The control of the false discovery rate in multiple testing under dependency. *The Annals of Statistics*, 29(4):1165–1188, 2001.
- Annalisa Buniello, Jacqueline A L MacArthur, Maria Cerezo, Laura W Harris, James Hayhurst, Cinzia Malangone, Aoife McMahon, Joannella Morales, Edward Mountjoy, Elliot Sollis, et al. The NHGRI-EBI GWAS Catalog of published genome-wide association studies, targeted arrays and summary statistics 2019. *Nucleic Acids Research*, 47(D1):D1005–D1012, 2019.
- Emmanuel J Candès, Yingying Fan, Lucas Janson, and Jinchi Lv. Panning for gold: ‘model-X’ knockoffs for high dimensional controlled variable selection. *Journal of the Royal Statistical Society: Series B (Statistical Methodology)*, 80(3):551–577, 2018.
- Stephen J Chanock, Teri Manolio, Michael Boehnke, Eric Boerwinkle, David J Hunter, Gilles Thomas, Joel N Hirschhorn, Goncalo Abecasis, David Altshuler, Joan E Bailey-Wilson, et al. Replicating genotype–phenotype associations. *Nature*, 447(7145):655–660, 2007.
- The International HapMap 3 Consortium. Integrating common and rare genetic variation in diverse human populations. *Nature*, 467(7311):52–58, 2010.
- David R Cox. A note on data-splitting for the evaluation of significance levels. *Biometrika*, 62(2):441–444, 1975.

- Bradley Efron, Trevor Hastie, Iain Johnstone, and Robert Tibshirani. Least angle regression. *The Annals of Statistics*, 32(2):407–499, 2004.
- William Fithian, Dennis Sun, and Jonathan Taylor. Optimal inference after model selection. *arXiv preprint arXiv:1410.2597*, 2014.
- Jerome Friedman, Trevor Hastie, Holger Höfling, and Robert Tibshirani. Pathwise coordinate optimization. *The Annals of Applied Statistics*, 1(2):302–332, 2007.
- Jerome Friedman, Trevor Hastie, and Robert Tibshirani. Regularization paths for generalized linear models via coordinate descent. *Journal of Statistical Software*, 33(1):1–22, 2010.
- Michael D Gallagher and Alice S Chen-Plotkin. The post-gwas era: from association to function. *The American Journal of Human Genetics*, 102(5):717–730, 2018.
- Jennifer E Huffman. Examining the current standards for genetic discovery and replication in the era of mega-biobanks. *Nature Communications*, 9(1):1–4, 2018.
- Jason D Lee, Dennis L Sun, Yuekai Sun, and Jonathan E Taylor. Exact post-selection inference, with application to the lasso. *The Annals of Statistics*, 44(3):907–927, 2016.
- Richard Lockhart, Jonathan Taylor, Ryan J Tibshirani, and Robert Tibshirani. A significance test for the lasso. *The Annals of Statistics*, 42(2):413–468, 2014.
- Nicolai Meinshausen and Peter Bühlmann. Stability selection. *Journal of the Royal Statistical Society: Series B (Statistical Methodology)*, 72(4):417–473, 2010.
- Nicolai Meinshausen, Lukas Meier, and Peter Bühlmann. P-values for high-dimensional regression. *Journal of the American Statistical Association*, 104(488):1671–1681, 2009.
- Alan J Miller. Selection of subsets of regression variables. *Journal of the Royal Statistical Society: Series A (General)*, 147(3):389–410, 1984.
- Alan J Miller. *Subset selection in regression*. CRC Press, 2002.
- Matteo Sesia, Chiara Sabatti, and Emmanuel J Candès. Gene hunting with hidden markov model knockoffs. *Biometrika*, 106(1):1–18, 2019.
- Rajen D Shah and Richard J Samworth. Variable selection with error control: another look at stability selection. *Journal of the Royal Statistical Society: Series B (Statistical Methodology)*, 75(1):55–80, 2013.
- John D Storey. The positive false discovery rate: a bayesian interpretation and the q-value. *The Annals of Statistics*, 31(6):2013–2035, 2003.
- Weijie Su, Małgorzata Bogdan, and Emmanuel J Candès. False discoveries occur early on the lasso path. *The Annals of Statistics*, 45(5):2133–2150, 2017.
- Zhan Su, Jonathan Marchini, and Peter Donnelly. Hapgen2: simulation of multiple disease snps. *Bioinformatics*, 27(16):2304–2305, 2011.
- Cathie Sudlow, John Gallacher, Naomi Allen, Valerie Beral, Paul Burton, John Danesh, Paul Downey, Paul Elliott, Jane Green, Martin Landray, et al. UK Biobank: an open access resource for identifying the causes of a wide range of complex diseases of middle and old age. *PLOS Medicine*, 12(3):e1001779, 2015.

- Robert Tibshirani. Regression shrinkage and selection via the lasso. *Journal of the Royal Statistical Society: Series B (Statistical Methodology)*, 58(1):267–288, 1996.
- Robert Tibshirani, Michael Saunders, Saharon Rosset, Ji Zhu, and Keith Knight. Sparsity and smoothness via the fused lasso. *Journal of the Royal Statistical Society: Series B (Statistical Methodology)*, 67(1):91–108, 2005.
- Ryan J Tibshirani, Jonathan Taylor, Richard Lockhart, and Robert Tibshirani. Exact post-selection inference for sequential regression procedures. *Journal of the American Statistical Association*, 111(514):600–620, 2016.
- Peter M Visscher, Naomi R Wray, Qian Zhang, Pamela Sklar, Mark I McCarthy, Matthew A Brown, and Jian Yang. 10 years of gwas discovery: biology, function, and translation. *The American Journal of Human Genetics*, 101(1):5–22, 2017.
- Larry Wasserman and Kathryn Roeder. High dimensional variable selection. *The Annals of Statistics*, 37(5A):2178–2201, 2009.
- David Williams. *Probability with martingales*. Cambridge University Press, 1991.
- Yujun Wu, Dennis D Boos, and Leonard A Stefanski. Controlling variable selection by the addition of pseudovariables. *Journal of the American Statistical Association*, 102(477):235–243, 2007.
- Hui Zou. The adaptive lasso and its oracle properties. *Journal of the American Statistical Association*, 101(476):1418–1429, 2006.
- Hui Zou and Trevor Hastie. Regularization and variable selection via the elastic net. *Journal of the Royal Statistical Society: Series B (Statistical Methodology)*, 67(2):301–320, 2005.